Acute Hepatobiliary Imaging

4

Marina C. Bernal Fernandez, Jorge A. Soto, and Christina A. LeBedis

Abstract

Abdominal pain is a common chief complaint in the emergency department, and computed tomography (CT) and ultrasound are useful first-line imaging modalities in the appropriate clinical setting. Both are rapid, low cost, and easily accessible. Magnetic resonance (MR) imaging is increasingly used in equivocal situations, especially for imaging the biliary system and pancreas, in the setting of pregnancy, and in young or relatively young patients with chronic diseases which will require multiple imaging examinations, with the associated exposure of ionizing radiation if repetitive CT is performed. MR has proved particularly useful in the setting of Crohn disease, complications of pancreatitis, suspected appendicitis in pregnant patients, complications from pancreatic injury, choledocholithiasis, and biliary obstruction of indeterminate etiology. Acute abdominal pain related to liver, gallbladder, and biliary etiologies may present as acute infections with hepatitis or cholecystitis, acute obstruction with choledocholithiasis or malignancy, hemoperitoneum from a ruptured liver mass, or trauma/iatrogenic injury.

M. C. Bernal Fernandez, M.D. • J. A. Soto, M.D. (✉)
C. A. LeBedis, M.D.
Department of Radiology, Boston University Medical Center, Boston, MA, USA
e-mail: Jorge.Soto@bmc.org

4.1 Acute Nontraumatic

Abdominal pain is a common chief complaint in the emergency department, and computed tomography (CT) and ultrasound are useful first-line imaging modalities in the appropriate clinical setting. Both are rapid, low cost, and easily accessible. Magnetic resonance (MR) imaging is increasingly used in equivocal situations, especially for imaging the biliary system and pancreas, in the setting of pregnancy, and in young or relatively young patients with chronic diseases which will require multiple imaging examinations, with the associated exposure of ionizing radiation if repetitive CT is performed. MR has proved particularly useful in the setting of Crohn disease, complications of pancreatitis, suspected appendicitis in pregnant patients, complications from pancreatic injury, choledocholithiasis, and biliary obstruction of indeterminate etiology. Acute abdominal pain related to liver, gallbladder, and biliary etiologies may present as acute infections with hepatitis or cholecystitis, acute obstruction with choledocholithiasis or malignancy, hemoperitoneum from a ruptured liver mass, or trauma/iatrogenic injury.

4.2 Liver

4.2.1 Acute Hepatitis

Acute hepatitis of any origin causes edema of the hepatocytes leading to injury. It can manifest as

M. Patlas et al. (eds.), *MDCT and MR Imaging of Acute Abdomen*,
https://doi.org/10.1007/978-3-319-70778-5_4

enlarged liver with no focal signs of disease on imaging. When present, symptoms may include fatigue, weakness, abdominal pain, hepatomegaly, and splenomegaly. Acute hepatitis remains a clinical diagnosis, with generally limited need for imaging evaluation. Etiologies include viral hepatitis—hepatitis A (fecal-oral transmission), hepatitis B and C (IV drug use, sex or blood transfusion transmission), and hepatitis D and E—and drug-induced hepatitis with alcohol or acetaminophen, as well as autoimmune, steatohepatitis, among others.

In acute hepatitis, ultrasound (US) may show either a normal liver or a decreased echogenicity of the parenchyma, and prominence of the portal venous system, which is commonly known as a "starry sky" appearance. In chronic hepatitis, the liver is echogenic. However, this is not specific for hepatitis, and may be seen with any chronic liver disease. Additional nonspecific ultrasound findings seen in hepatitis include gallbladder wall thickening, contraction, and periportal lymphadenopathy. Hepatitis B and C increase the risk of cirrhosis, portal hypertension, and hepatocellular carcinoma. Coarse echotexture and surface nodularity are more specific signs of cirrhosis on US. CT and MR play a limited role in evaluating acute hepatitis, but may show nonspecific findings including hepatomegaly and periportal edema or enhancement [1]. MR may show heterogeneous liver intensity on T2-weighted images, and immediately after intravenous contrast administration. In the setting of equivocal liver enzyme elevation with nonspecific symptoms in a patient suspected of having steatohepatitis, MR

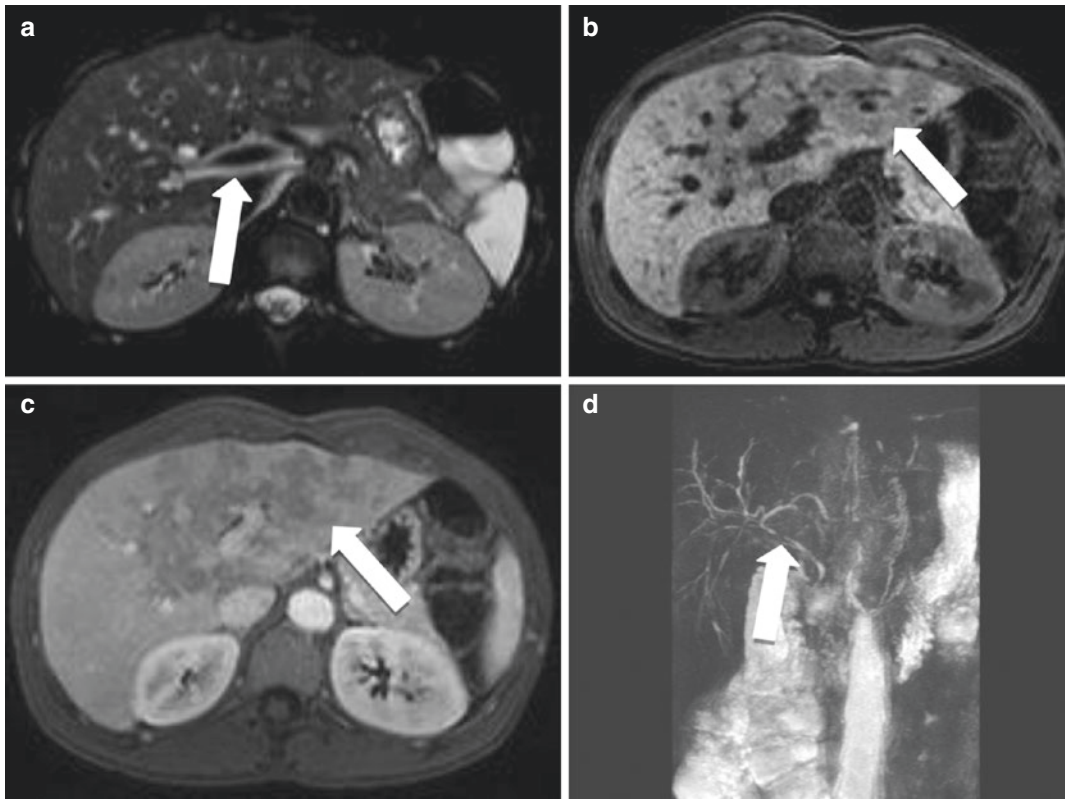

Fig. 4.1 AIDS cholangiohepatitis. 26-year-old man with AIDS and acute transaminitis of unknown etiology. Axial T2-weighted fat-saturated MR image (**a**) shows periportal edema (arrow). Axial T1-weighted fat-saturated pre-contrast (**b**) and post-contrast MR images in the portal venous phase (**c**) demonstrate heterogeneous hepatic parenchymal enhancement (arrow), a nonspecific finding which can be seen in the setting of hepatitis. 3D MRCP image (**d**) reveals multifocal segmental strictures of the intra- and extrahepatic biliary tract (arrow), which given the clinical information is highly consistent with AIDS cholangiopathy

is the examination with the most sensitivity and specificity. MR hepatic perfusion abnormalities may be seen in active liver disease, or in extrinsic inflammatory processes which have blood drainage to the liver, including pancreatitis and bowel inflammatory diseases (Figs. 4.1 and 4.2) [2].

4.2.2 Perihepatitis/Fitz-Hugh-Curtis Syndrome

Fitz-Hugh-Curtis syndrome is characterized by right-sided abdominal pain and perihepatitis due to pelvic inflammatory disease from a variety of organisms, particularly chlamydia and gonorrhea. Infection ascends from the vagina or cervix to the endometrium, fallopian tubes, and contiguous structures, resulting in endometritis, salpingitis, and tubo-ovarian abscess, which, if left untreated, may spread along the right paracolic gutter, resulting in perihepatitis. Typical findings include stringlike adhesions between the anterior surface of the liver and the parietal peritoneum, which are seen on US, CT, or MR as thickening and abnormal enhancement of the anterior liver capsule with peritoneal septations and loculated perihepatic ascites (Fig. 4.3) [3]. Nonspecific findings also include inflammation in the hepatorenal fossa, and gallbladder wall thickening. Clinical history and clinical examination pointing to pelvic inflammatory disease are essential to consider the diagnosis.

4.2.3 Hepatic Abscess

An abscess is a localized collection of necrotic inflammatory tissue caused by bacteria, fungal species, or parasites. Pyogenic liver abscesses usually develop secondary to an intestinal source of bacteria, as with appendicitis or diverticulitis, from recent surgery, or from complications of blunt or penetrating trauma. Clinical presentation is usually insidious, with several days to weeks of low-grade fever and right upper quadrant pain. Complications of liver abscess which may present with acute pain and/or sepsis include subphrenic abscess, peritoneal rupture, and Budd-Chiari syndrome from compression of the inferior vena cava or hepatic veins. Laboratory analysis shows leukocytosis, anemia, and elevated ESR.

US shows complex fluid collections of mixed echogenicity, thick-walled cysts, or cysts with fluid-fluid levels. An abscess may also appear as a solid liver mass, at which time through transmission aids in identifying them as nonsolid [4]. CT or MR may be needed for further characterization. CT demonstrates a peripherally enhancing, centrally hypoattenuating well-defined mass. A "double-target sign" may be seen with a hypodense fluid center, a hyperdense inner ring representing an abscess membrane which persists on delayed imaging, and a hypodense outer ring representing liver edema which only enhances on delayed images. MR classically shows a mass which is hypointense on T1-weighted images, hyperintense on T2-weighted images with thick walls, and internal septations which enhance on early arterial-phase imaging, and demonstrates persistent enhancement on late-phase imaging. An abscess will also show diffusion restriction (Figs. 4.4 and 4.5). MR is useful when a mass is not definitively characterized using CT, as MR gadolinium chelates have a higher sensitivity than CT does using iodinated contrast [5]. Differentiating an abscess from a metastasis with a large necrotic component may be difficult. In the setting of a metastasis, MR may show more progressive, centripetal stromal enhancement, and may have a more nodular, irregular, and thicker rim with a necrotic metastasis than with an abscess.

Fungal abscess may occur in immunocompromised patients, and most commonly caused by *Candida albicans* which concomitantly infects the spleen. Nodules are usually numerous, subcapsular, and small, measuring less than 1 cm. CT may show the classic target nodule in smaller form and peripheral distribution, but often does not show these characteristics convincingly enough to establish definitive diagnosis due to their small size and peripheral distribution. MR sequences with dynamic gadolinium-enhanced gradient-echo and T2-weighted fat-suppressed sequences are more sensitive for the identification of hepatosplenic candidiasis [6, 7]. Chronic

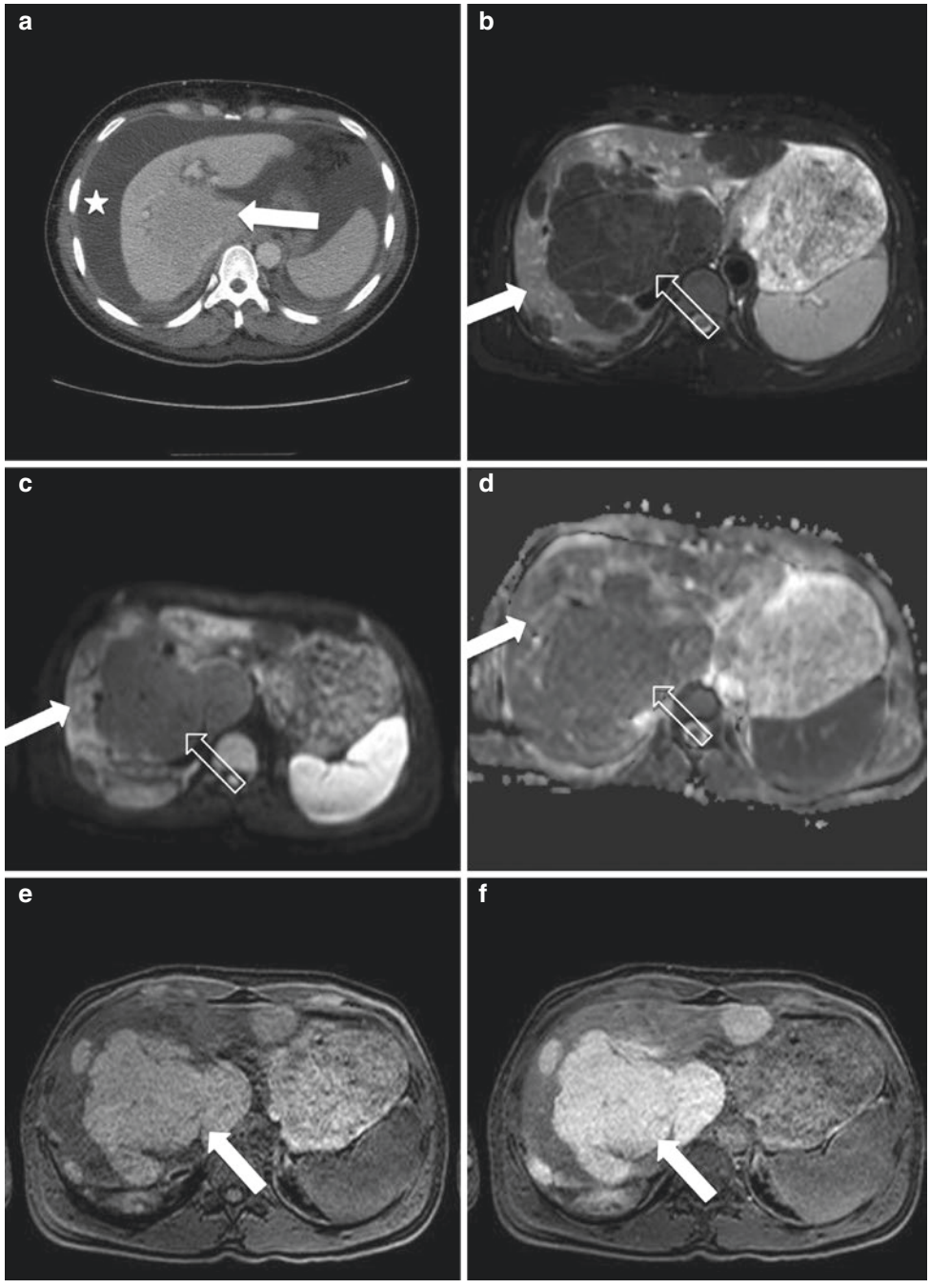

Fig. 4.2 Acute hepatic insult with subsequent nodular regenerative hyperplasia. 38-year-old man with elevated bilirubin, elevated INR, new ascites, and weight loss. Axial IV contrast-enhanced CT image (**a**) demonstrates extensive ascites (star) and a markedly abnormal liver with central hypoenhancement (arrow) and peripheral enhancement which was concerning for a mass. A follow-up MRI was obtained 6 weeks later. Axial T2-weighted fat-saturated MR image (**b**) and B600 diffusion-weighted MR image (**c**) reveal that the periphery of the liver has hyperintense signal (arrows) which does not restrict on the ADC map (arrow, **d**) while the central liver and scattered round foci at the periphery are normal (open arrow on the dominant nodule). T1-weighted fat-saturated pre-contrast (**e**) and 10-min-delay post-contrast (**f**) MR images reveal multiple regenerative nodules, particularly in the central liver (arrow on the dominant nodule), with large regions of hypoenhancement at the periphery of the liver. These findings were sequelae of the acute hepatic insult of unknown etiology that the patient sustained at the time of presentation, and not a tumor

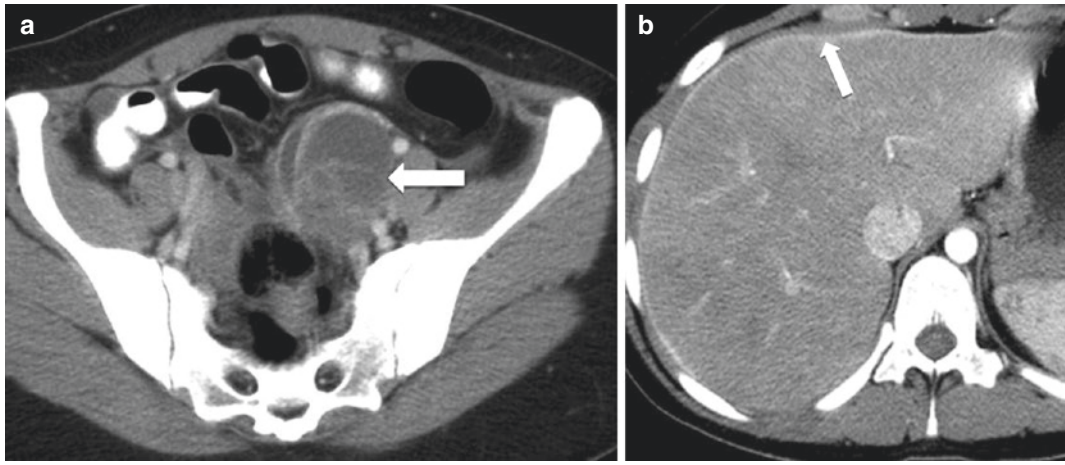

Fig. 4.3 Fitz-Hugh-Curtis syndrome. 25-year-old woman with cervical motion tenderness and right upper quadrant pain. (**a**) Contrast-enhanced axial CT image of the pelvis demonstrates a multi-loculated cyst in the left ovary, consistent with a tubo-ovarian abscess (arrow). (**b**) IV contrast-enhanced axial CT image of the upper abdomen demonstrates capsular enhancement of the liver (arrow), representing perihepatitis. Together, these findings represent Fitz-Hugh-Curtis syndrome

nodules may be seen as irregular shaped foci which are hypointense on T1-weighted images and isointense on T2-weighted images, with negligible enhancement, as they represent scar tissue.

Amebic abscesses result from primary colonic involvement with *Entamoeba histolytica* with seeding through the portal venous drainage, and hence affecting the right hepatic lobe, more commonly. It is thought that abscesses may result from trophosite obstruction in small venules, causing ischemic necrosis and infection [8]. These are indistinguishable from pyogenic abscess, but are more often seen as single masses and in a subdiaphragmatic location, with a thick 5–10 mm capsule which enhances (Fig. 4.6). Complications include intraperitoneal rupture with subsequent peritonitis, and diaphragmatic invasion with pulmonary consolidation and empyema. Conservative medical treatment is effective in most cases, with percutaneous drainage reserved for larger abscesses and abscesses close to the heart.

Other parasitic infections of the liver include echinococcal disease, which presents as a multicystic liver abscess with multiple daughter cysts, and schistosomiasis with ova infecting the portal triads, and causing fibrosis seen as thickened echogenic triads.

4.2.4 Portal Vein Thrombosis/ Occlusion

Portal vein thrombosis or occlusion results from either slow flow as in portal hypertension or post-surgery, hypercoagulable states, or intestinal infection/inflammation including appendicitis or pancreatitis, as well as from external compression from tumors or lymphadenopathy. Thrombosis may be well tolerated with no acute symptoms, or may present as acute abdominal pain or variceal bleeding.

US shows an intraluminal filling defect which varies in echogenicity. On color Doppler, flow void or complete lack of intraluminal flow is seen. Sensitivity and specificity are close to 90% [9]. False positive causes include slow portal vein flow. False negative causes include a large periportal collateral which can be confused with a patent portal vein. In the setting of chronic portal vein thrombosis, cavernous transformation is seen as multiple collateral vessels surrounding a thrombosed portal vein (Fig. 4.7).

MR is useful in distinguishing tumor thrombus from bland thrombus and in patients with equivocal US findings. Diagnosis is best achieved by combining black-blood techniques (spin-echo techniques with superior and inferior saturation pulses) or bright-blood technique

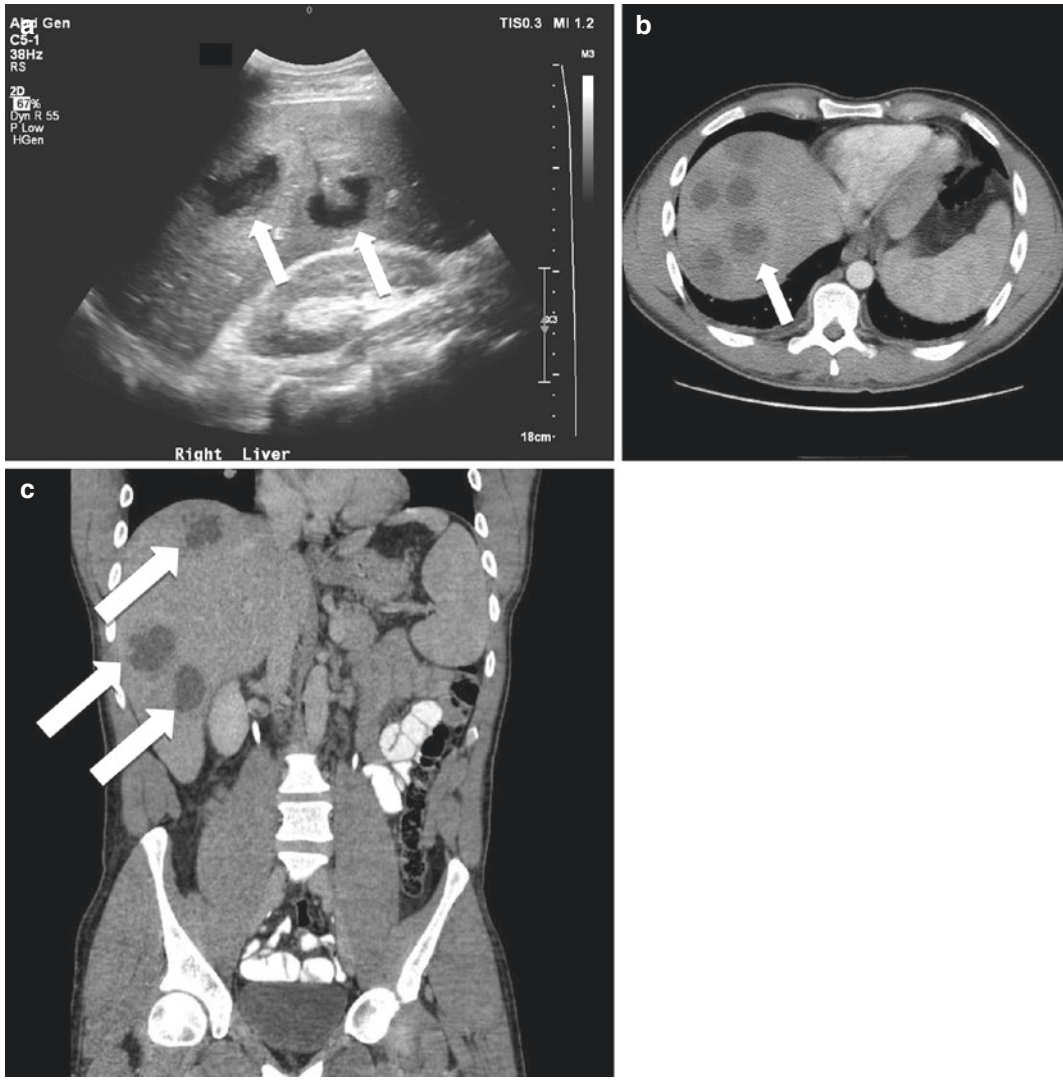

Fig. 4.4 Liver abscesses. 43-year-old man with acute right upper quadrant pain and elevated GGT. Representative longitudinal image from an ultrasound through the liver (**a**) demonstrates multiple hypoechoic hepatic masses with peripheral echogenic rims (arrows). Axial (**b**) and coronal (**c**) IV contrast-enhanced CT images reveal multiple peripherally enhancing, centrally hypoattenuating masses in the liver (arrows), consistent with hepatic abscesses, which were of mixed flora at pathologic analysis via image-guided drainage

(time-of-flight (TOF) gradient echo (GRE) or gadolinium-enhanced gradient echo) [10]. Tumor thrombus is most commonly seen with hepatocellular carcinoma, and shows high signal on T2-weighted images and soft-tissue signal intensity on TOF GRE images, and enhances with intravenous gadolinium. Bland thrombus is seen in cirrhosis, infection, or inflammation, and is low in signal on T2-weighted images and TOF, and does not enhance with gadolinium. If bland thrombus is infected, one may see enhancement of the portal vein wall.

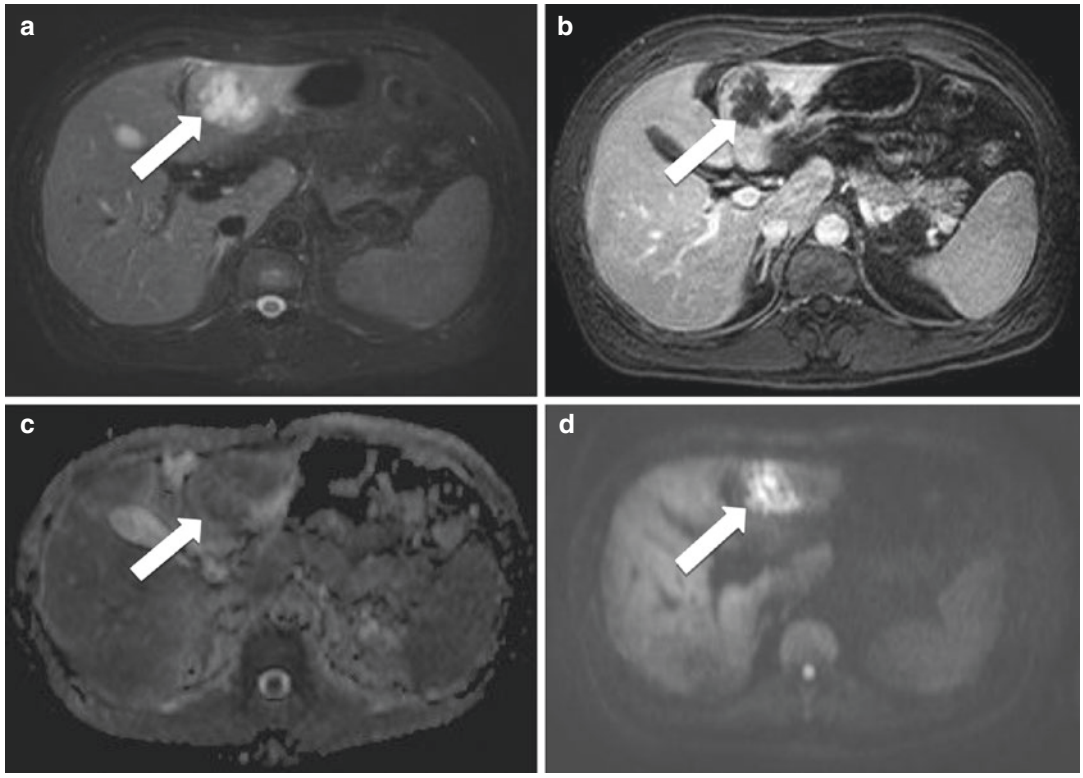

Fig. 4.5 Liver abscess. 45-year-old man with elevated bilirubin, fever, and leukocytosis. Axial T2 fat-saturated image through the liver (**a**) demonstrates an irregular hyperintense mass in segment three (arrow). Axial T1-weighted post-contrast MR image (**b**) in the equilibrium phase shows peripheral enhancement and central hypointensity of this mass, while ADC map (**c**) and B600 (**d**) MR images reveal restricted diffusion in this mass (arrows). Percutaneous sampling proved this to be a *Klebsiella pneumoniae* liver abscess

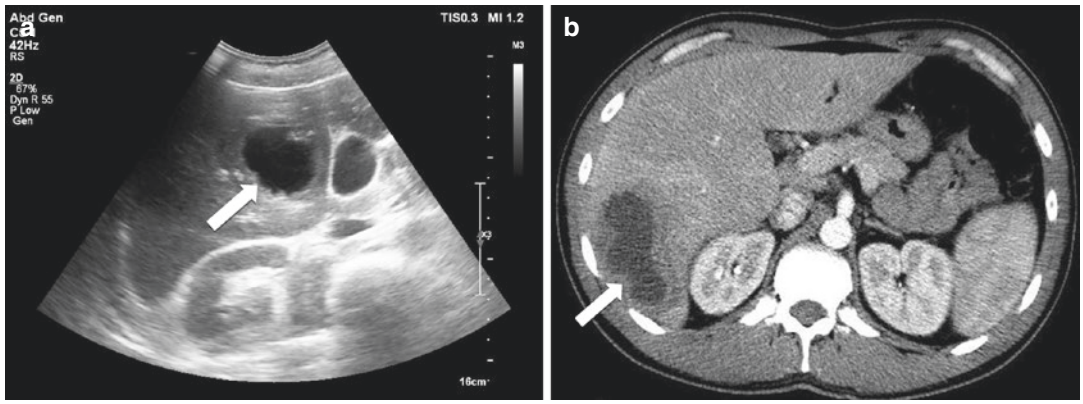

Fig. 4.6 Amebic abscess. 35-year-old woman with abdominal pain, fevers, and chills. Grayscale axial ultrasound image (**a**) demonstrates a large irregular thick-walled cyst in the right hepatic lobe (arrow). Axial IV contrast-enhanced CT image (**b**) reveals a rim-enhancing low-attenuation mass with peripheral edema (arrow) in segment six and associated hyperemia, which proved to be an amebic abscess

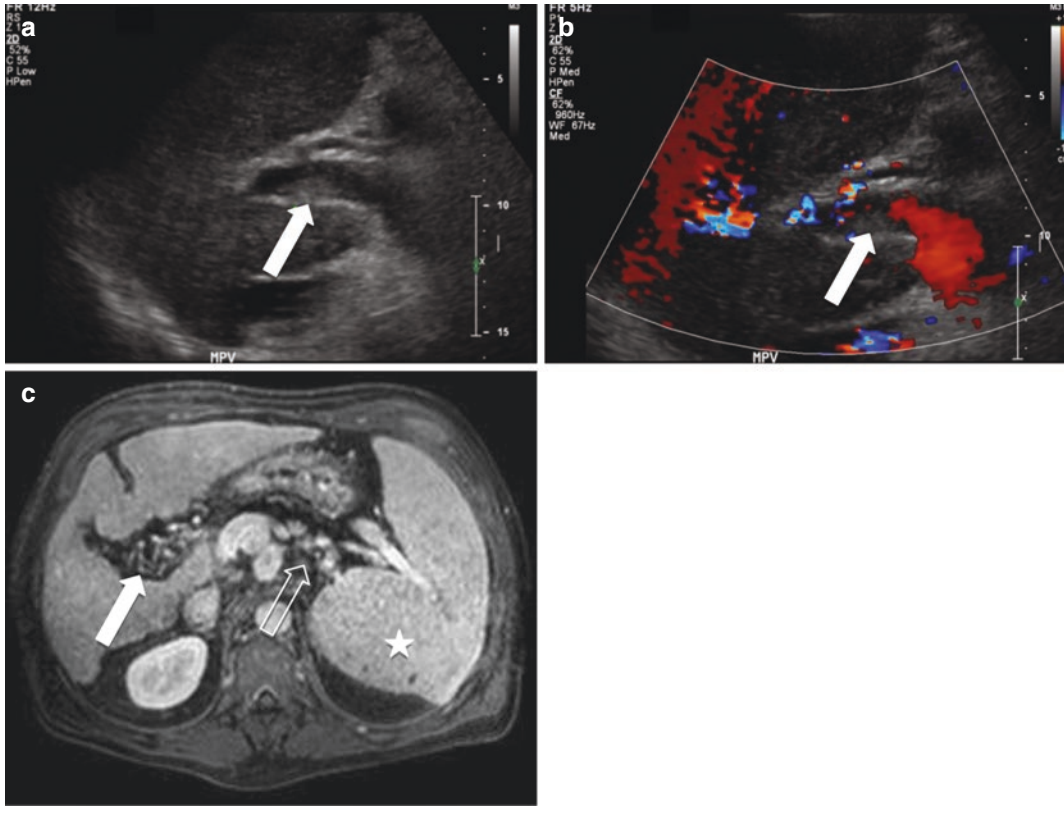

Fig. 4.7 Portal vein thrombosis. 53-year-old man with a history of hepatitis C-related cirrhosis. 2D (**a**) and color Doppler (**b**) longitudinal ultrasound images acquired 8 years prior demonstrate a nonocclusive thrombus (arrows) in the main portal vein. Recent T1-weighted post-contrast axial MR image (**c**) demonstrates cavernous transformation in the porta hepatis (solid arrow) due to interval complete portal vein occlusion since the prior ultrasound. Note is also made of mild splenomegaly (star) and splenorenal shunts (open arrow)

4.2.5 Budd-Chiari Syndrome

Budd-Chiari syndrome is characterized by centrilobular congestion, hepatocellular necrosis, and atrophy from hepatic venous outflow obstruction due to IVC or hepatic vein thrombosis. Common causes of thrombosis include pregnancy, oral contraceptive use, polycythemia vera, chronic fibrosis, webs obstructing the veins, and tumors including HCC, renal cell carcinoma, and adrenal cortical carcinoma. Patients may present clinically with abdominal pain, signs of portal hypertension, and ascites. CT and MR findings in acute Budd-Chiari syndrome include narrowing or non-visualization of the hepatic veins and/or IVC, caudate lobe enlargement, decreased peripheral parenchymal enhancement, and intrahepatic collateral vessels which may be seen as comma-shaped enhancing vessels (Fig. 4.8) [11].

4.2.6 Hepatic Infarction

Because of the dual arterial and portal blood supply to the liver, hepatic infarcts are very uncommon. Hepatic infarction is a grave complication most often seen after liver transplantation, often necessitating repeat transplantation. Acute hepatic infarction appears hypoechoic on US and hypoattenuating on CT. A key imaging feature of hepatic infarction is the preservation of portal tracts, because it differentiates it from other etiologies, including abscess, biloma, and post-biopsy hematoma. A potential pitfall is focal

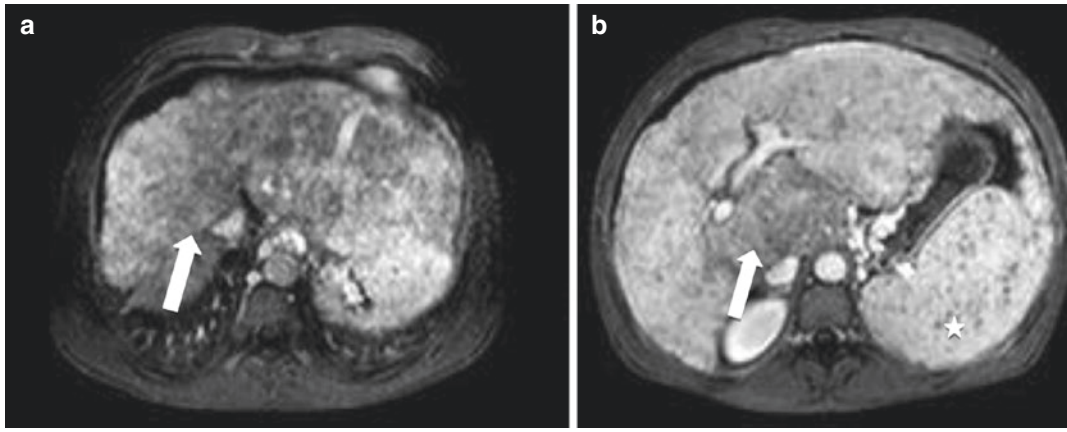

Fig. 4.8 Budd-Chiari syndrome. 26-year-old man from Sudan with a history of giardiasis and amebic infections. T1-weighted post-contrast axial MR image in the portal venous phase (**a**) shows occlusion of the hepatic veins (arrow) in the enlarged and nodular liver. Delayed enhancement of the peripheral liver with central low density and hypertrophy of the caudate lobe (arrow, **b**) is noted on an axial T1-weighted MR image, which is highly consistent with Budd-Chiari syndrome. Note is also made that the spleen is borderline enlarged (star, **b**)

hepatic steatosis. However, this tends to occur in characteristic locations, and normally enhancing vessels course through it [12].

4.2.7 Hepatocellular Carcinoma

Patients with hepatitis or any type of chronic liver disease are at increased risk of hepatocellular carcinoma (HCC). Prevalence is highest in Asia and Africa due to higher rates of viral hepatitis. Nonetheless, incidence has been steadily increasing in the United States. Any liver mass in a patient with chronic liver disease should be further evaluated with dedicated liver imaging, with either a multiphase contrast-enhanced CT liver mass protocol or a dynamic contrast-enhanced MR liver mass protocol. There is consensus that MR is superior to CT for the identification of HCC [13]. US has a sensitivity of 60% and a specificity of 85–90% for the diagnosis of HCC, and is easily accessible and uses no ionizing radiation, hence its use as the primary screening modality. Recent literature has shown the potential usefulness of MR as a screening modality for patients with chronic liver disease at risk of HCC, due to its higher sensitivity and specificity [14].

HCC is the fifth most common malignancy in the world, and accounts for one million deaths annually, with a 5-year survival rate of <5% for untreated, symptomatic HCC [15]. For tumors >2 cm, MR most frequently shows hyperintensity on T2-weighted images and hypointensity on T1-weighted images, with enhancement on arterial phase images, washout on portal venous and delayed images, and late pseudocapsular enhancement (Fig. 4.9). Although usually asymptomatic, HCC may present in the emergency setting as hemoperitoneum from a ruptured mass. Different mechanisms have been described, including tumor expansion leading to subcapsular hemorrhage, and rupture of the liver capsule with associated intraperitoneal hemorrhage. This may present clinically as sudden onset of epigastric or right hypochondrial pain due to Glisson's capsule distention, peritonitis, hypotension, and shock from bleeding. A clinical history of cirrhosis or HCC is essential, or high suspicion in a patient from an endemic area with acute abdominal pain.

CT findings include high-attenuation peritoneal fluid around the liver and spleen in the setting of acute bleeding from a ruptured mass, with change in composition and, hence, density of the hematoma, depending on the age of the blood products, clotting, and layering hematocrit effect [16]. Small volumes of blood may layer in Morrison's pouch or in the pelvis. A classic CT finding, the "sentinel clot"

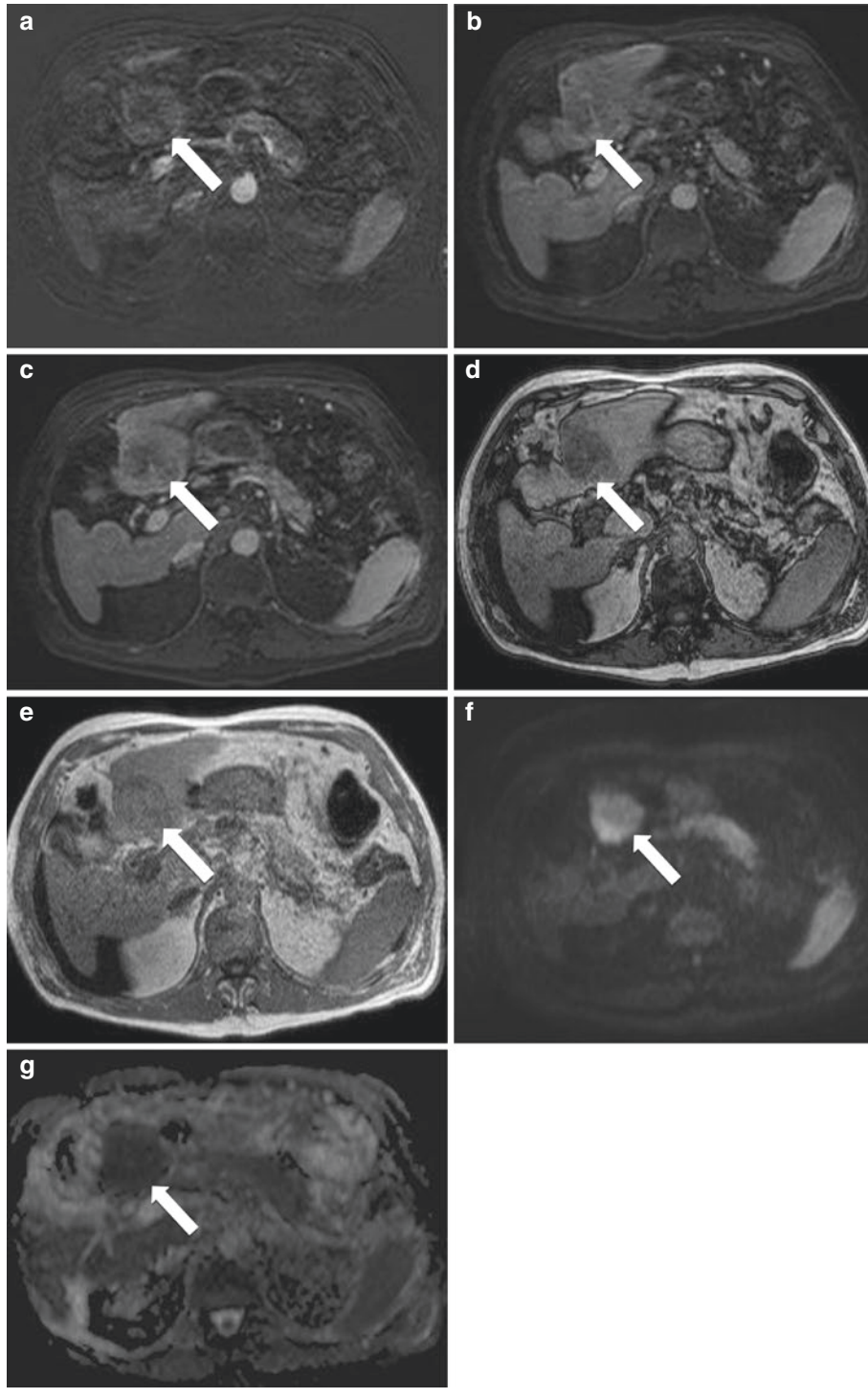

Fig. 4.9 Hepatocellular carcinoma. 79-year-old man with cirrhosis and liver masses detected incidentally on a chest CT done for rectal cancer staging. Axial MR images demonstrate cirrhosis, perihepatic ascites, and a 5.5 cm mass in segment three with arterial enhancement (arrow, **a**), and washout on venous and equilibrium phase T1-weighted fat-saturated images (arrows, **b** and **c**, respectively), signal loss on T1-weighted out-of-phase (arrow, **d**) when compared to T1-weighted in-phase imaging (arrow, **e**), and restricted diffusion on B600 (arrow, **f**) when compared to the ADC map (arrow, **g**), which is highly consistent with a well-differentiated hepatocellular carcinoma

sign, which refers to clotted blood at the site of tissue rupture, which usually has Hounsfield units of 45–60 (Figs. 4.10 and 4.11). Blood spilling into the peritoneal cavity will show Hounsfield units (HU) of acute blood at approximately 45 HU. Mortality is high, and urgent treatment is needed with transcatheter arterial embolization. MR findings are similar to those seen on CT, with signal characteristics of blood varying based on the age of the blood products. By the time most patients get imaged, the majority of the blood products will be high signal on T1-weighted imaging, and mixed or intermediate signal on T2-weighted images [15].

4.2.8 Hepatic Adenoma

Hepatocellular adenoma is a mass composed of normal hepatocytes which produce bile but do not have bile ductules, and are partially or completely enclosed by a pseudocapsule from compressed hepatic parenchyma. It used to be a rare tumor until the introduction of oral contraceptives [17]. Other causes include diabetes, glycogen storage disease, iron overload, and anabolic steroids. Although usually asymptomatic and diagnosed incidentally, patients may present with acute abdominal pain related to intratumoral hemorrhage or, rarely, peritoneal

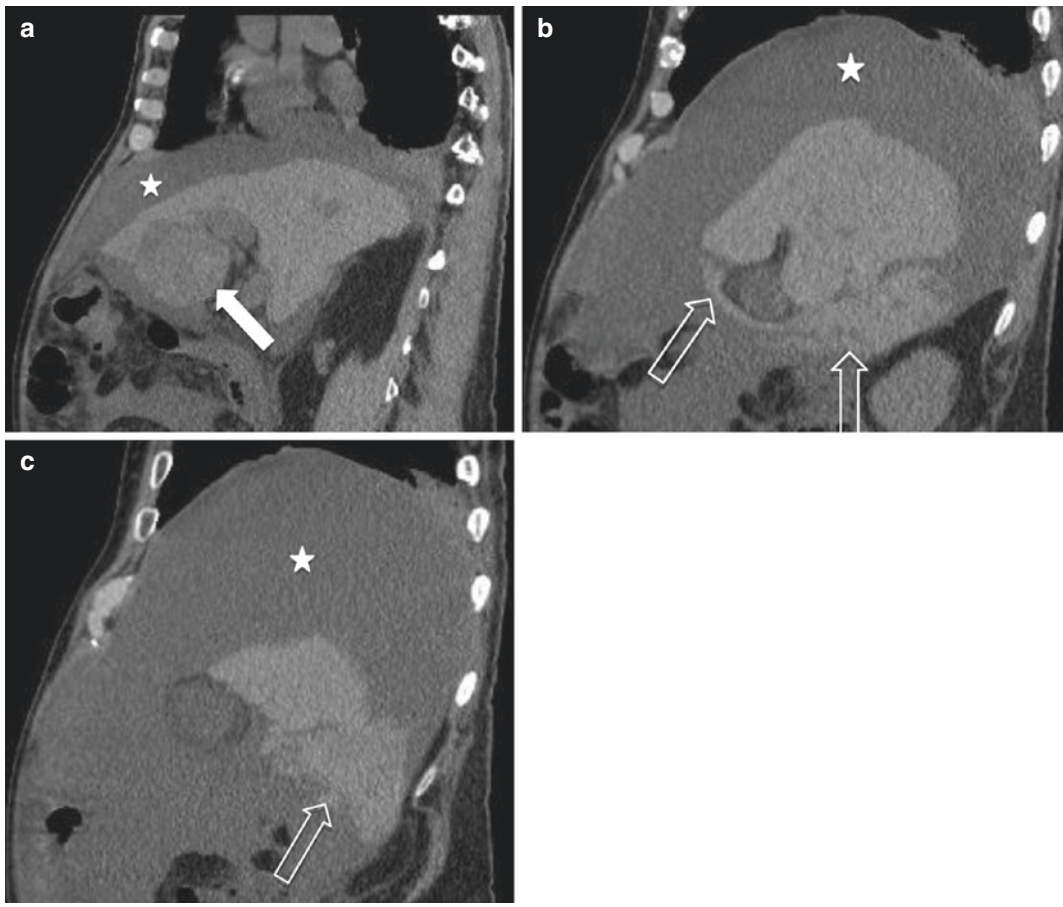

Fig. 4.10 Same patient as in Fig. 4.9. Ruptured hepatocellular carcinoma. 79-year-old man with known hepatocellular carcinoma diagnosed 3 months ago presents with an acute hematocrit drop and grossly bloody ascites on paracentesis after a fall 1 day prior. Sagittal non-contrast CT images demonstrate the known segment three hepatocellular carcinoma (arrow, **a**) and adjacent sentinel clot (open arrows, **b** and **c**) tracking into the right paracolic gutter. Extensive hemoperitoneum is noted (star)

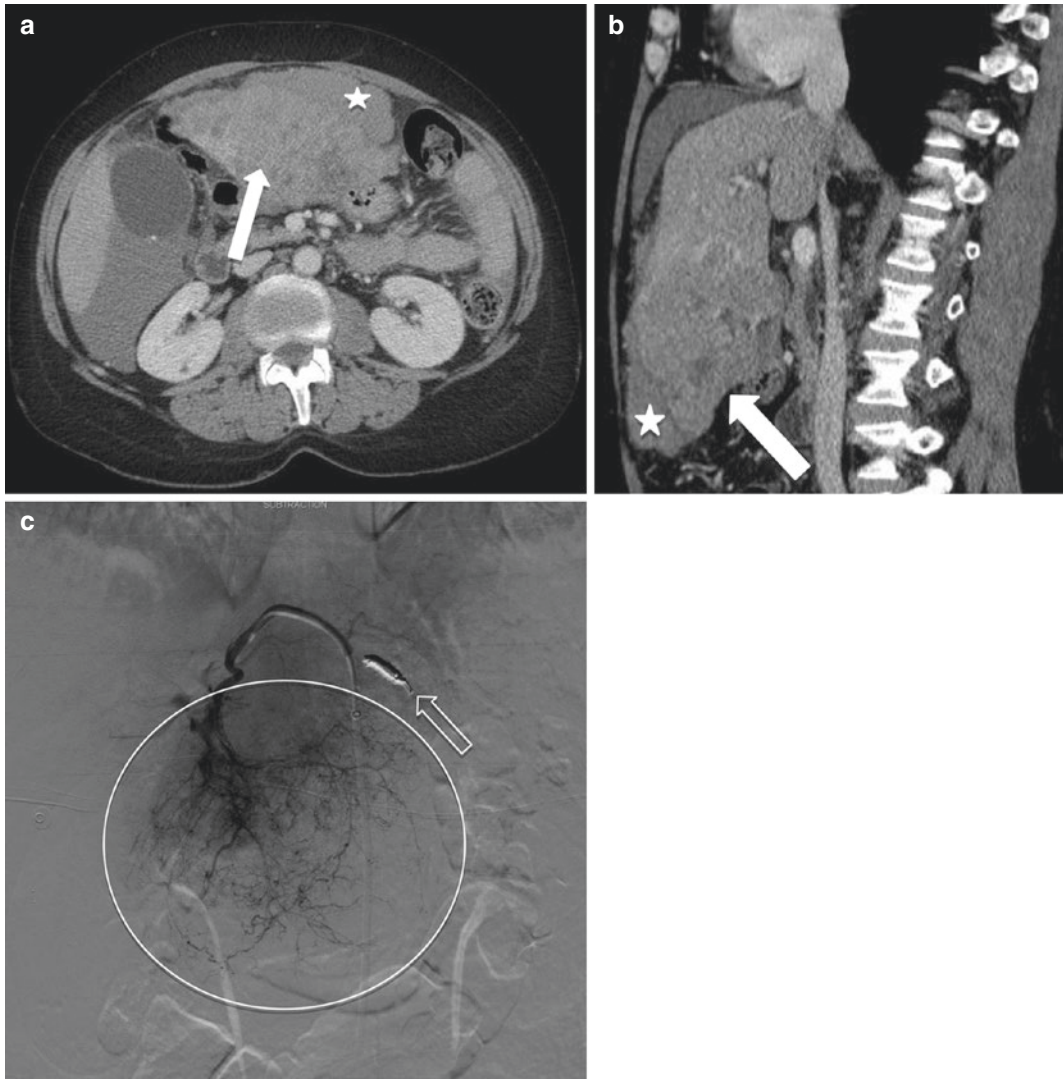

Fig. 4.11 Ruptured hepatocellular carcinoma with subsequent embolization. 54-year-old man with chronic hepatitis C, cirrhosis, and ascites presented with tachycardia and abdominal pain. Axial (**a**) and sagittal (**b**) IV contrast-enhanced CT images show a large heterogeneous mass (arrows) in the left lobe of a cirrhotic liver, with adjacent active hemorrhage (star), representing a ruptured hepatocellular carcinoma. Simple perihepatic ascites is also visualized. Digital subtraction angiographic image (**c**) reveals a large hypervascular tumor arising from the left lobe of the liver (circle). This mass derived its blood supply from a replaced left hepatic artery arising from the left gastric artery. To avoid nontarget embolization of the lesser curvature of the stomach, a large branch of the left gastric artery was embolized using two metallic coils (open arrow). Subsequent bland embolization of the hepatocellular carcinoma was performed

hemorrhage requiring emergent intervention. Malignant transformation is rare.

Because US findings are nonspecific, showing a single mass of variable echogenicity, additional imaging is usually needed for diagnosis. On non-v CT, adenomas are usually isodense to liver, or hypodense if they contain fat (Fig. 4.12). If there is hemorrhage, non-contrast CT shows areas of high attenuation, or heterogeneity if there is old hemorrhage. Intratumoral hemorrhage is seen in 25–40% of adenomas (Fig. 4.13) [18]. If intravenous contrast is given, early homogeneous enhancement

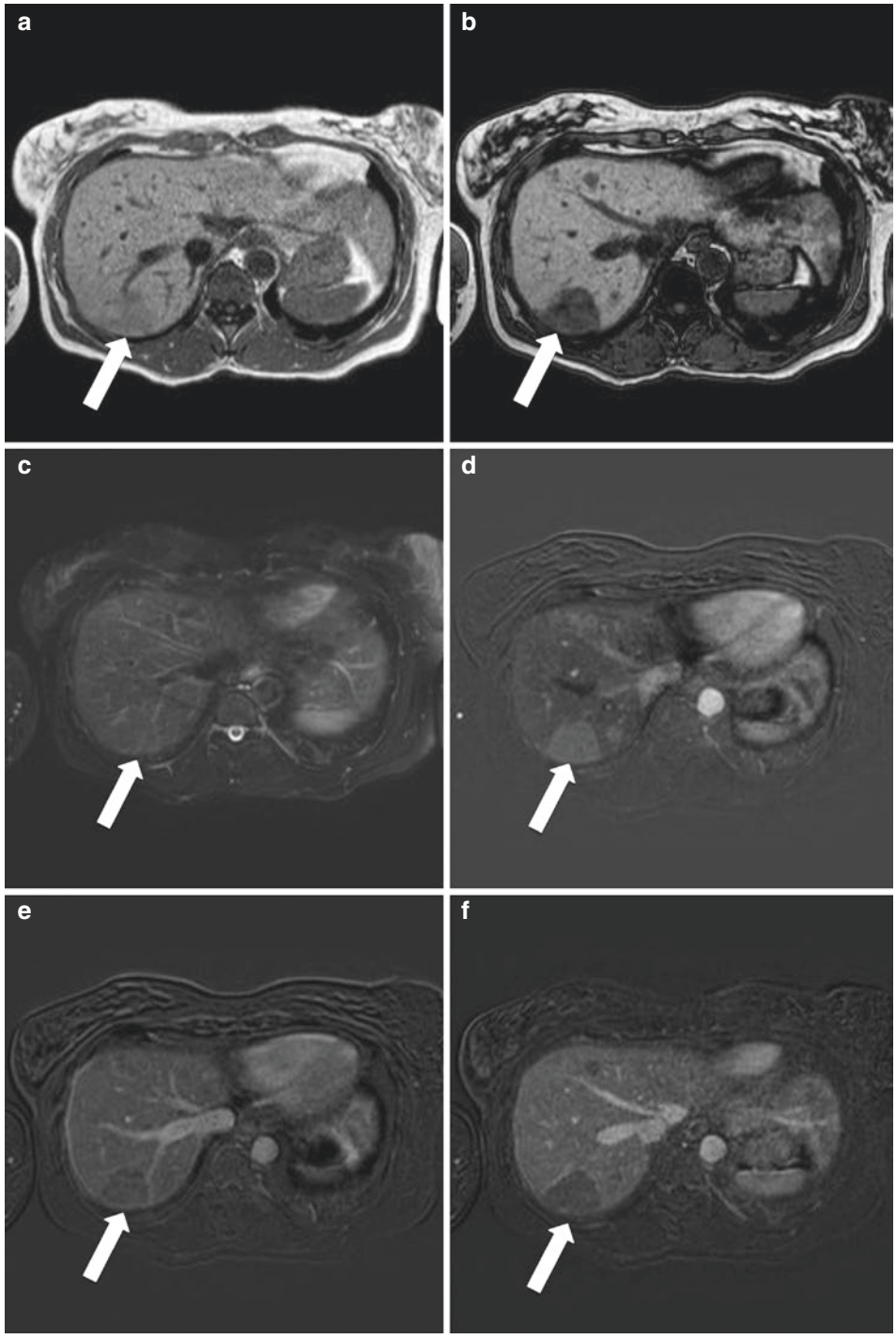

Fig. 4.12 Hepatic adenoma. 51-year-old woman with biopsy-proven hepatic adenomatosis. These masses were incidentally detected on a CT scan of her thorax when she was 36 years old. The largest of the patient's known hepatic adenomas is shown in segment seven on MR imaging. In-phase (**a**) and opposed-phase (**b**) T1-weighted MR images reveal signal loss on the opposed-phase image, consistent with intratumoral fat. This mass is only faintly T2 hyperintense on this T2-weighted fat-saturated image (**c**). Dynamic post-contrast subtraction images reveal arterial enhancement (**d**) followed by rapid wash-out on the venous phase (**e**), and pseudocapsular enhancement on the equilibrium phase (**f**), classic imaging features for a hepatic adenoma in a non-cirrhotic patient

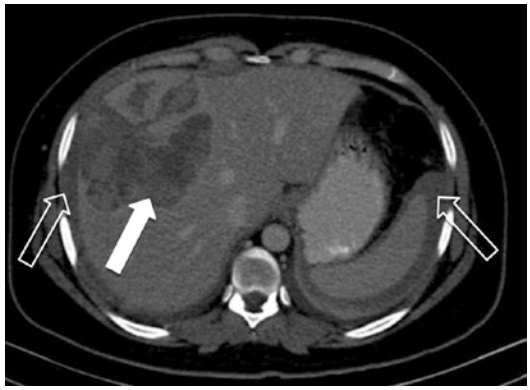

Fig. 4.13 Ruptured hepatic adenoma. 28-year-old woman with a known hepatic adenoma who presents with new-onset acute abdominal pain. Axial IV contrast-enhanced CT image reveals hyperattenuation within the known hepatic adenoma, representing acute hemorrhage (closed arrow). Associated hemoperitoneum is visualized (open arrow)

and isodensity with liver parenchyma in portal venous and delayed phases are seen. Non-bleeding masses are usually managed conservatively if they measure less than 5 cm [19].

MR shows a homogeneous mass with mild hyperintensity on T2-weighted images and hypo- or isointensity on T1-weighted images. Post-contrast images show a transient homogeneous blush which uniformly fades to isointensity with normal liver parenchyma by 1 min [20]. More heterogeneous signal may be seen on T1- and T2-weighted images depending on the amounts of fat, hemorrhage, and necrosis. When the mass shows an intense marble pattern of arterial enhancement, it may be difficult to distinguish it from HCC, but the presence of washout and a capsule in HCC should help make the distinction.

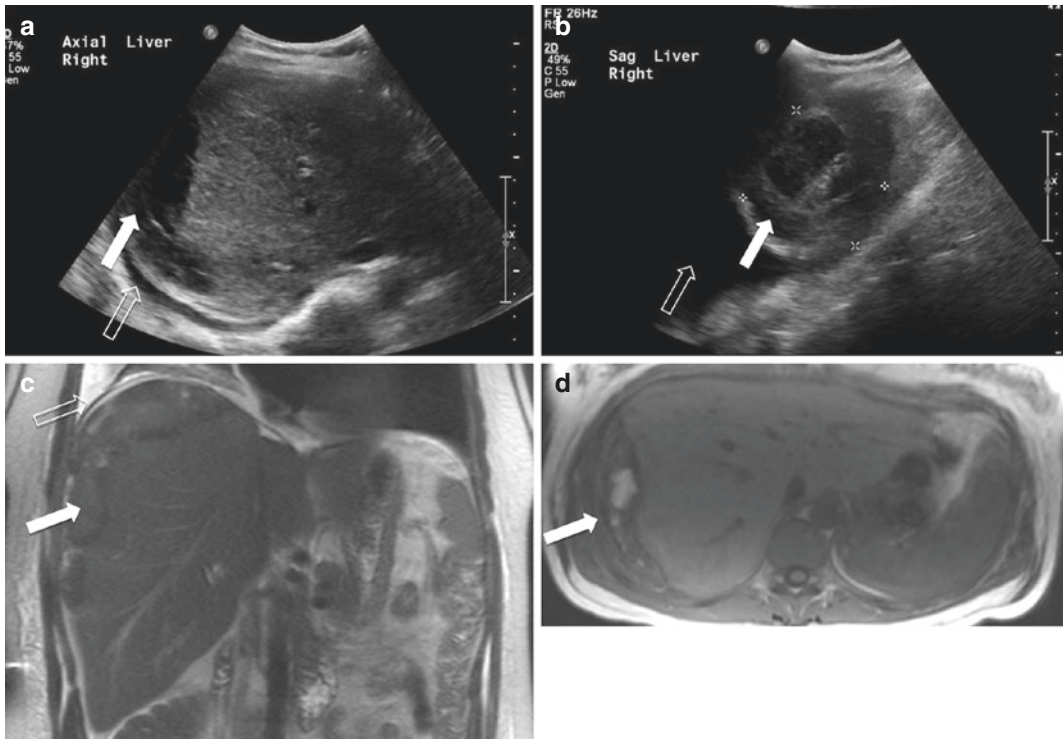

Fig. 4.14 HELLP syndrome. 36-year-old pregnant woman with elevated liver function tests and right upper quadrant pain. Axial (**a**) and longitudinal (**b**) grayscale ultrasound images of the liver demonstrate a heterogeneous perihepatic fluid collection (solid arrows) as well as a right pleural effusion (open arrows). Coronal T2-weighted (**c**) and axial T1-weighted (**d**) images confirm the presence of perihepatic hematoma (solid arrows) in this patient with HELLP syndrome. The right pleural effusion is also seen in C (open arrow) (images courtesy of Dr. Vincent Mellnick)

4.2.9 HELLP Syndrome

HELLP syndrome is an uncommon but serious obstetrical condition characterized by hemolysis (H), elevated liver enzymes (EL), and low platelet count (LP), and occurs in 0.2–0.6% of all pregnancies, and in 10–20% of women with severe preeclampsia [21, 22]. Maternal clinical symptoms are nonspecific and, unfortunately, can masquerade as a variety of other conditions. The pathophysiology of HELLP has not been clearly elucidated to our knowledge; however, altered placental function resulting in ischemia-producing oxidative stress is one proposed etiology [23]. Imaging features of HELLP include perihepatic free fluid, hepatic steatosis, liver enlargement, and a periportal halo which may precede more severe conditions including hepatic hematoma and hepatic rupture with hemoperitoneum (Fig. 4.14), leading to high morbidity and mortality [24].

4.3 Gallbladder

4.3.1 Acute Calculous Cholecystitis

The most common cause of acute cholecystitis is impacted calculi in the cystic duct or common bile duct (95%) [25]. Calculi obstruct bile drainage into the common bile duct, leading to gallbladder overdistention, increased intraluminal pressure, inflammation, and eventually wall ischemia and bacterial superinfection with necrosis, if not treated promptly. Clinical presentation includes a history of colicky pain after a meal of high-fat content, with acute onset of constant, right upper quadrant pain lasting >6 h, with or without fever, chills, and laboratory markers of acute inflammation including leukocytosis. US is the first-line modality for diagnosis, showing cholelithiasis, diffuse wall thickening with pericholecystic fluid and/or hyperemia, gallbladder distention greater than 10 × 4 cm, and a positive sonographic Murphy sign [26].

When initial findings are indeterminate and clinical examination is not definitive for acute cholecystitis, hepatobiliary scintigraphy, CT, or MRI may be used for definitive diagnosis prior to surgery. MR is particularly useful for identifying a different cause for the patient's symptoms, and for identifying a cause for biliary obstruction when calculi are not seen. CT is 85% sensitive for gallstones, less than US, but may show additional findings of stranding of the pericholecystic fat, abnormalities in the gallbladder fossa, and complications including gas in the gallbladder wall as is seen in emphysematous cholecystitis [27]. Additionally, if narrow CT windows are used and/or newer techniques such as dual energy, the yield of CT increases to higher than the aforementioned 85% [28].

A more comprehensive evaluation of cholecystitis, its root cause, and possible complications is achieved with MR. The high sensitivity of T1-weighted fat-saturated contrast-enhanced images makes MR an excellent tool for the diagnosis of cholecystitis, with sensitivity greater than that of ultrasound [29]. Findings are similar to those seen on CT, with mucosal enhancement on early phases, and progressive gallbladder wall enhancement and transient enhancement of surrounding liver parenchyma. On T2-weighted imaging, calculi can be excluded or identified, and pericholecystic fluid and abscesses are revealed if present. MR in conjunction with MRCP increases sensitivity for the diagnosis of exclusion of coexisting choledocholithiasis, can reveal a mass or another cause of obstruction including as stricture, and outlines possible complications, including empyema, perforation, and gangrene, which are not as readily seen on US, CT, or hepatobiliary scintigraphy (Fig. 4.15).

4.3.2 Acute Acalculous Cholecystitis

Acalculous cholecystitis accounts for approximately 5–10% of patients with acute cholecystitis, and has a higher mortality rate than calculous cholecystitis (approaching 50%), and a higher rate of complications including gangrene, emphysema, and perforation [26]. One must consider acute acalculous cholecystitis in patients with prolonged hospitalization, patients with comorbidities includ-

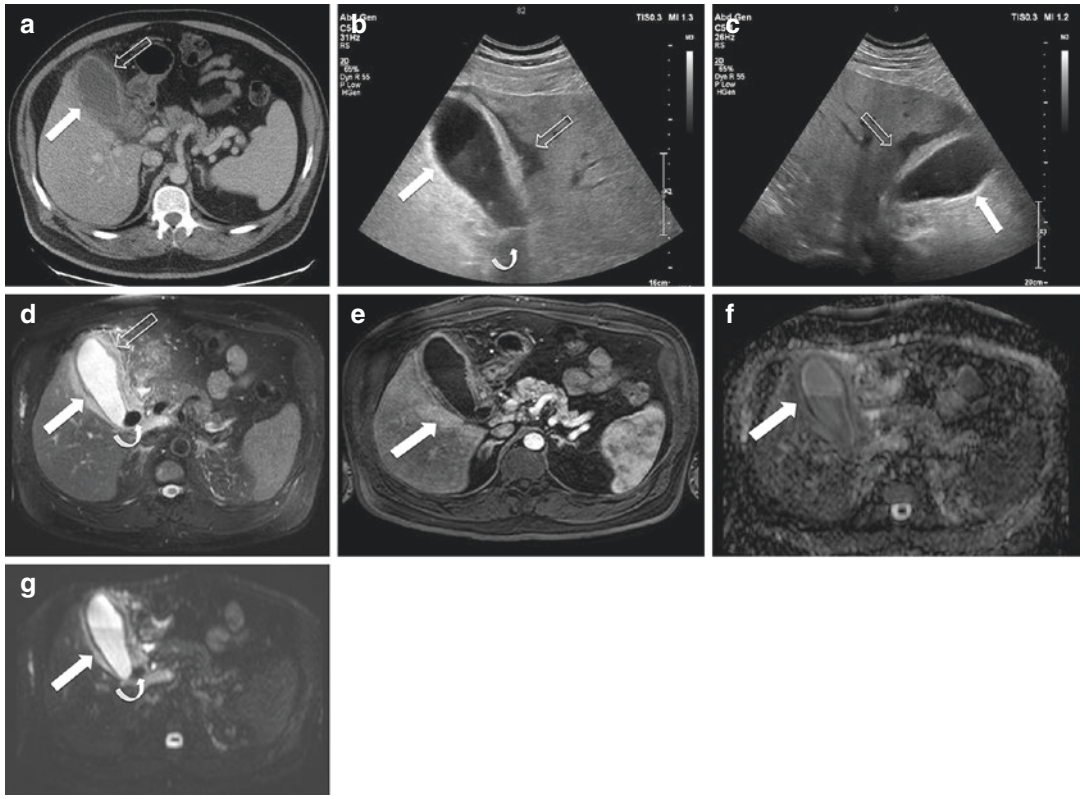

Fig. 4.15 Acute calculous cholecystitis. 53-year-old man with fever and leukocytosis. In the emergency department, an IV contrast-enhanced CT was acquired due to the absence of localizing symptoms. An axial CT image (**a**) demonstrates a distended gallbladder with wall thickening (arrow) and pericholecystic fluid and inflammation (open arrow), which is highly consistent with acute cholecystitis. Subsequent axial (**b**) and longitudinal (**c**) ultrasound images confirmed these findings (solid arrows and open arrows) and also identified a shadowing gallstone (curved arrow). An IV contrast-enhanced MRCP was performed to assess for possible choledocholithiasis and associated findings prior to cholecystectomy. T2-weighted fat-saturated axial image (**d**) again shows gallbladder distention, wall thickening (arrow), calculus (curved arrow), and pericholecystic fluid (open arrow). T1-weighted IV contrast-enhanced arterial phase MR image (**e**) demonstrates gallbladder fossa hyperemia (arrow). ADC (**f**) and B600 (**g**) axial MR images illustrate restricted diffusion of the gallbladder wall edema (arrows) and the calculus (curved arrow)

ing diabetes and sepsis, and patients undergoing mechanical ventilation or parenteral nutrition. Inflammation is not due to cystic duct obstruction, but rather wall ischemia from decreased gallbladder contraction and overdistention, or by direct bacterial infection. Clinical examination is similar to that of acute calculous cholecystitis, but is often masked by other comorbidities.

US, CT, and MR findings of acalculous cholecystitis include a distended gallbladder with wall thickening, intraluminal sludge with no calculi, pericholecystic fluid, and hyperemia of the gallbladder fossa on the arterial phase at CT or MR (Fig. 4.16). These findings are nonspecific, and may be seen with hypoalbuminemia, hepatitis, cirrhosis, and heart failure, making diagnosis difficult. Hepatobiliary scintigraphy may help to confirm the diagnosis by showing non-filling of the gallbladder, but may not reveal the cause for non-filling. MR with MRCP can be used to exclude choledocholithiasis, with a reported negative predictive value of 93% for a normal MRCP, and a probability of 89% of having no CBD calculus demonstrated as well as no readmission due to calculus disease within 6 months following MRCP [30]. MR/MRCP may reduce the amount of unnecessary ERCP procedures and associated complications.

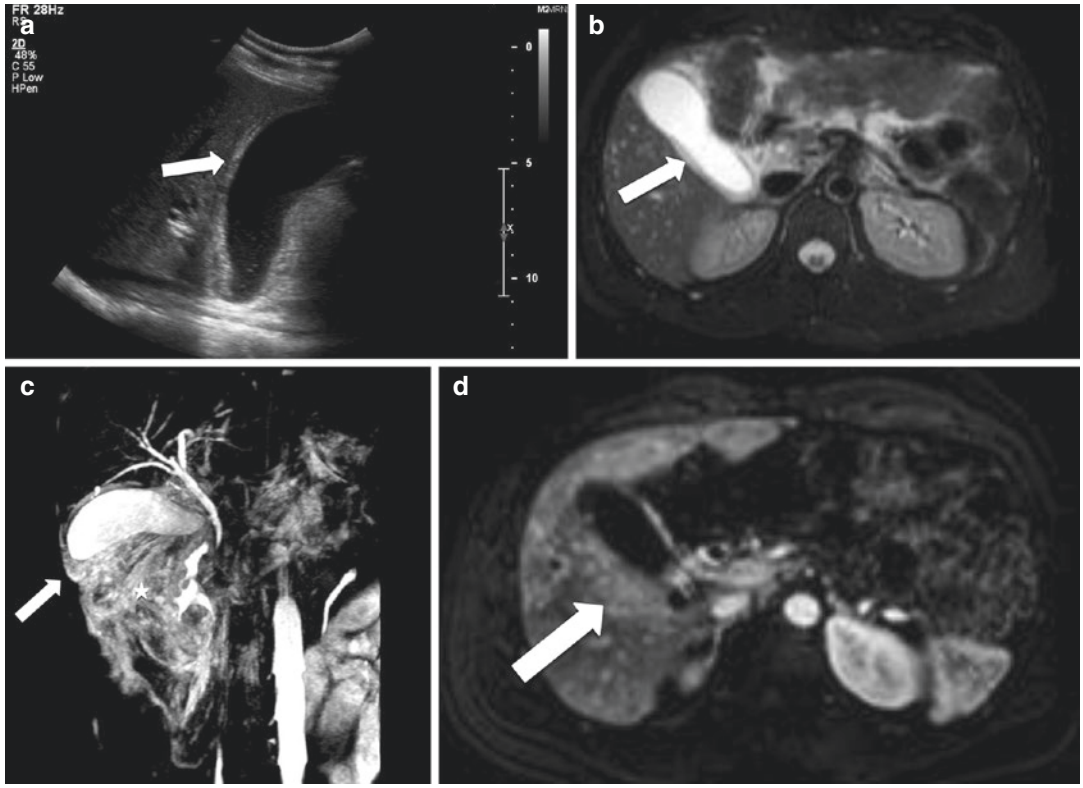

Fig. 4.16 Acute acalculous cholecystitis. 37-year-old man with right upper quadrant pain. Longitudinal ultrasound image (**a**) demonstrates distention and wall thickening of the gallbladder with associated pericholecystic fluid (arrow). No calculi are present. MR/MRCP was subsequently performed to assess for possible choledocholithiasis. Axial T2-weighted fat-saturated MR and 3D MRCP images (**b**, **c**) mirror the ultrasound, with gallbladder distention and wall thickening (arrows) with associated pericholecystic fluid (star on 3D MRCP image). Again, no calculi were seen. T1-weighted axial fat-saturated IV contrast-enhanced arterial phase MR image (**d**) shows hyperemia of the gallbladder fossa (arrow)

4.3.3 Complicated Acute Cholecystitis

Untreated acute cholecystitis may result in perforation, abscess formation, fistula, peritonitis, and gangrenous or emphysematous cholecystitis.

In gangrenous cholecystitis, there is necrosis of the gallbladder wall, which is a surgical emergency. US findings most specific for acute gangrenous cholecystitis include a striated, multilayered appearance of the gallbladder wall, and an irregular gallbladder wall with decreased or absent flow on Doppler [31]. CT and MR show intraluminal membranes, an indistinct wall with non-enhancement of the foci of gangrene, intraluminal blood contents, and pericholecystic abscess (Fig. 4.17) [32].

Emphysematous cholecystitis results from small-vessel ischemia resulting in gallbladder wall inflammation and necrosis with superinfection with gas-forming organisms. This entity is usually seen in diabetic or elderly patients, and carries a high mortality. Gallbladder wall gas is a specific sign readily seen on US and CT (Fig. 4.18). MR may become useful if the diagnosis is unclear, as it can show characteristic signal voids in the gallbladder wall or susceptibility artifact on GRE images. Although the cross-sectional imaging features of gangrenous and emphysematous cholecystitis overlap, the end result is still ischemia and necrosis, with an urgent need for appropriate management.

Additional complications from acute cholecystitis are perforation and/or hemorrhage of

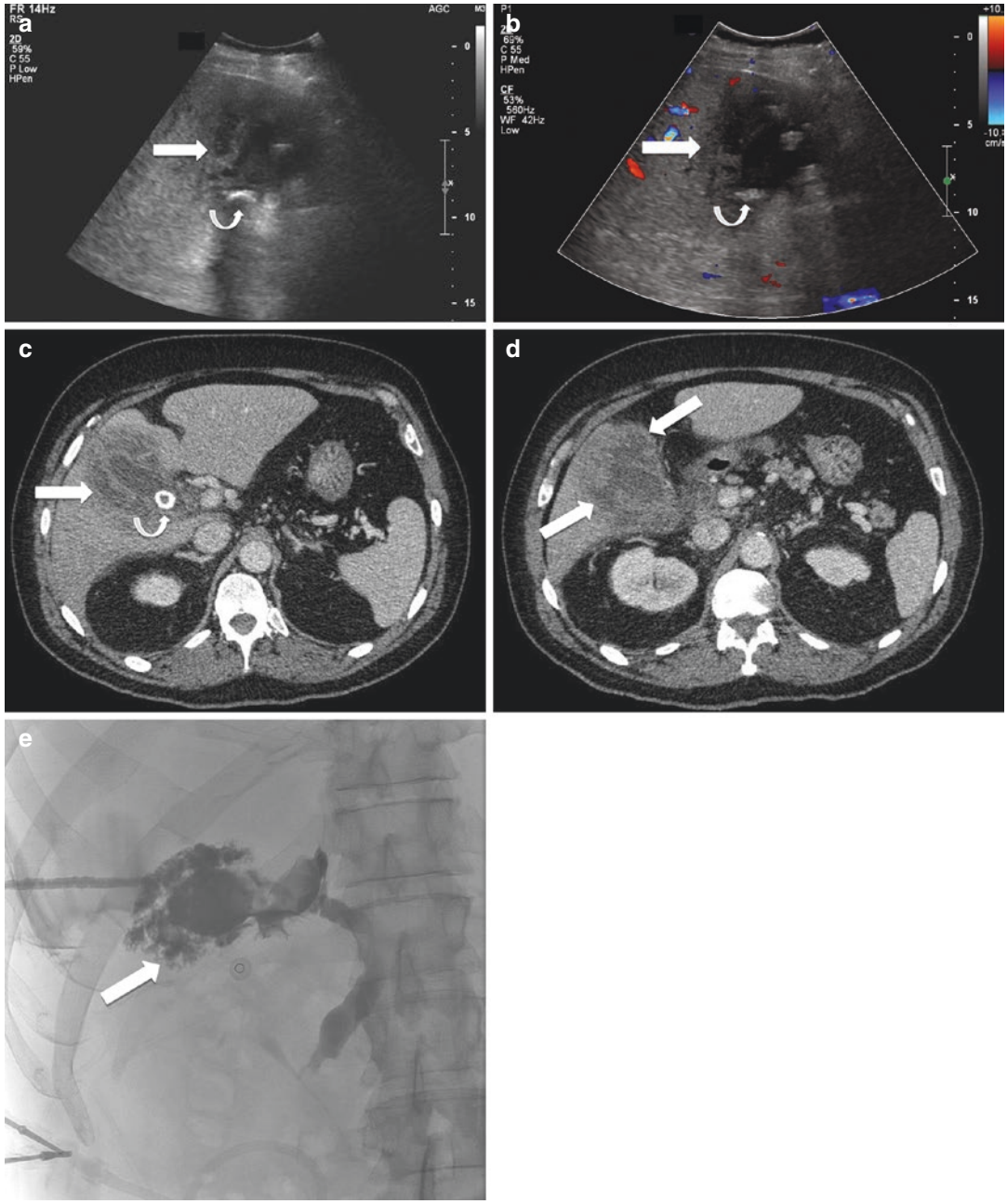

Fig. 4.17 Gangrenous cholecystitis. 70-year-old man with new liver function test elevation and fever. Grayscale (**a**) and color Doppler axial ultrasound images (**b**) reveal a markedly abnormal gallbladder which contains a calculus (curved arrows), and which has an irregular, thickened wall with associated pericholecystic fluid collections (arrows). Axial IV contrast-enhanced CT images (**c**, **d**) show similar findings; however, the discontinuity of the gallbladder wall is more conspicuous (arrows in **d**). A percutaneous cholecystostomy tube was placed, and at a later date a fluoroscopy tube check was performed (**e**), which demonstrates a patent cystic duct and a markedly abnormal gallbladder with a discontinuous wall and opacification of multiple pericholecystic fluid collections (arrow)

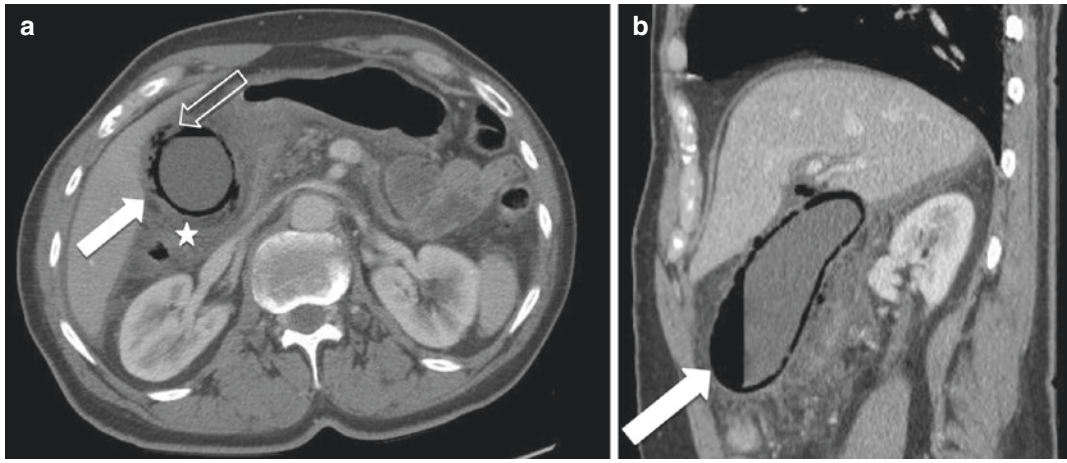

Fig. 4.18 Emphysematous cholecystitis. 74-year-old man with a history of metastatic non-small-cell lung cancer who presented to the emergency department with abdominal pain and vomiting. Axial (**a**) and sagittal (**b**) IV contrast-enhanced CT images reveal a distended gallbladder with a large amount of gas within its irregular wall and lumen (arrows). Multiple foci of discontinuity are seen in the gallbladder wall (open arrow, **a**), with dissection of free gas into the portocaval region (not shown). There was moderate perihepatic free fluid (star). There was a small amount of pneumobilia in the left hepatic lobe (not shown)

the gallbladder. Imaging findings in perforation include discontinuity of the gallbladder wall, bulging of the wall suggesting an underlying defect, and a pericholecystic fluid collection. MR imaging with T1-weighted post-gadolinium images and T2-weighted fat-suppressed images may be particularly useful when the perforation is discrete. Hemorrhage may be seen in CT as hyperattenuating blood, or in MR as T1 hyperintense signal as a result of the T1-shortening effect of methemoglobin [33].

4.4 Biliary Ducts

4.4.1 Choledocholithiasis

Choledocholithiasis is the most common cause of biliary obstruction, and may result in pancreatitis, jaundice, biliary colic, or cholangitis. Calculi lodged in the common bile duct most commonly form in the gallbladder and migrate to the CBD, are dislodged during cholecystectomy, or, rarely, may form in intrahepatic bile ducts and travel to the CBD (5%) [34]. Clinical presentation of choledocholithiasis ranges from mild to severe depending on the degree of obstruction and the presence of concomitant superinfection leading to cholangitis, which requires emergent drainage. Common symptoms include acute right upper quadrant pain, pruritus, and jaundice, with increased serum alkaline phosphatase and direct bilirubin levels. Common complications other than cholangitis include pancreatitis and secondary biliary cirrhosis.

The sensitivity of US for calculi in the central bile ducts ranges from 55 to 91% [35], with particular limitations due to duodenal gas artifact adjacent to the pancreatic head. A calculus is seen as an echogenic focus with posterior acoustic shadowing (Fig. 4.19). Ten percent of calculi may produce no acoustic shadowing. Associated US findings include biliary duct dilation, >6 mm for the common bile duct (age-appropriate adjustments must be taken into account), and >2 mm for the intrahepatic bile ducts. CT sensitivities range from 70 to 80%, and may show an intraductal calculus (usually calcified in up to 80%), with a rim of surrounding bile (meniscus

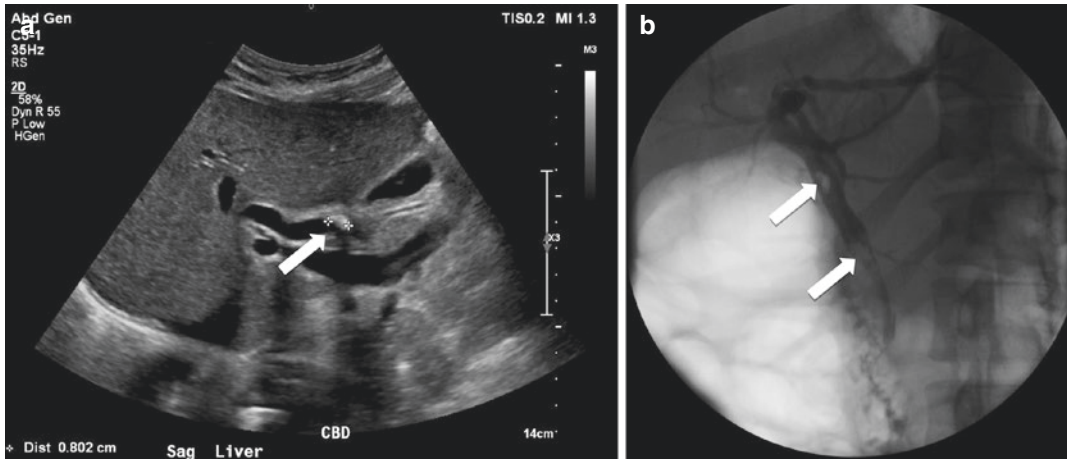

Fig. 4.19 Choledocholithiasis. 34-year-old woman with abnormal liver function tests. Longitudinal ultrasound image (**a**) demonstrates a shadowing calculus in the dilated common bile duct (arrow). Therapeutic ERCP (**b**) performed the next day shows two calculi in the common bile duct (arrows)

or bull's eye sign). Pure cholesterol calculi may not be seen, as they have the same density as bile. Indirect signs include biliary duct dilation, with abrupt termination of the CBD.

MRCP is commonly performed when only indirect signs are seen on ultrasound and/or CT where other diagnoses cannot be excluded, including CBD obstruction from pancreatic or ampullary malignancy, chronic pancreatitis, cholangiocarcinoma, stenosis or stricture from a variety of causes, and primary sclerosing cholangitis. MRCP has a sensitivity and specificity approaching 100%. Signs on MRCP include a low signal-dependent filling defect in the CBD (Fig. 4.20). It is imperative to review the source images, to avoid potential pitfalls including motion artifact, cholecystectomy clip susceptibility, and vascular compression, among others. The location of the filling defect is essential, as nondependent filling defects are seen in the setting of pneumobilia. When the diagnosis is not definitive on US, CT, or MRCP, ERCP is commonly performed, as it provides both diagnostic and therapeutic options, and is the imaging reference standard.

4.4.2 Acute (Ascending) Cholangitis

Acute cholangitis is characterized by the triad of right upper quadrant pain, fever, and jaundice, and is caused by gram-negative bacteria superinfecting bile in the common bile duct. It is most commonly seen in the setting of biliary tract obstruction, for which CT is most readily used to determine the cause. Eighty percent of biliary obstructions are due to choledocholithiasis, while the remaining are usually due to malignancy, sclerosing cholangitis, or biliary procedures including ERCP. US shows thickening of wall of bile duct with debris (usually pus) in the common bile duct and associated intra- and/or extrahepatic biliary duct dilation. Urgent antibiotics with gram-negative coverage and biliary decompression are potentially lifesaving. If severe, mortality rates have been reported up to 50–90%. CT and MR are useful to determine the cause of cholangitis when a calculus is not readily seen on US, and when the diagnosis is not clinically evident. Early, inhomogeneous arterial enhancement of the liver is seen in CT, although this finding is nonspecific. T1-weighted fat-suppressed post-gadolinium MR images show thickened bile duct walls with increased enhancement. T2-weighted MR images may show ill-defined periportal hyperintense signal from inflammation, and wedge-shaped hyperintense regions of infection (Fig. 4.21). These findings also help in distinguishing primary sclerosing cholangitis.

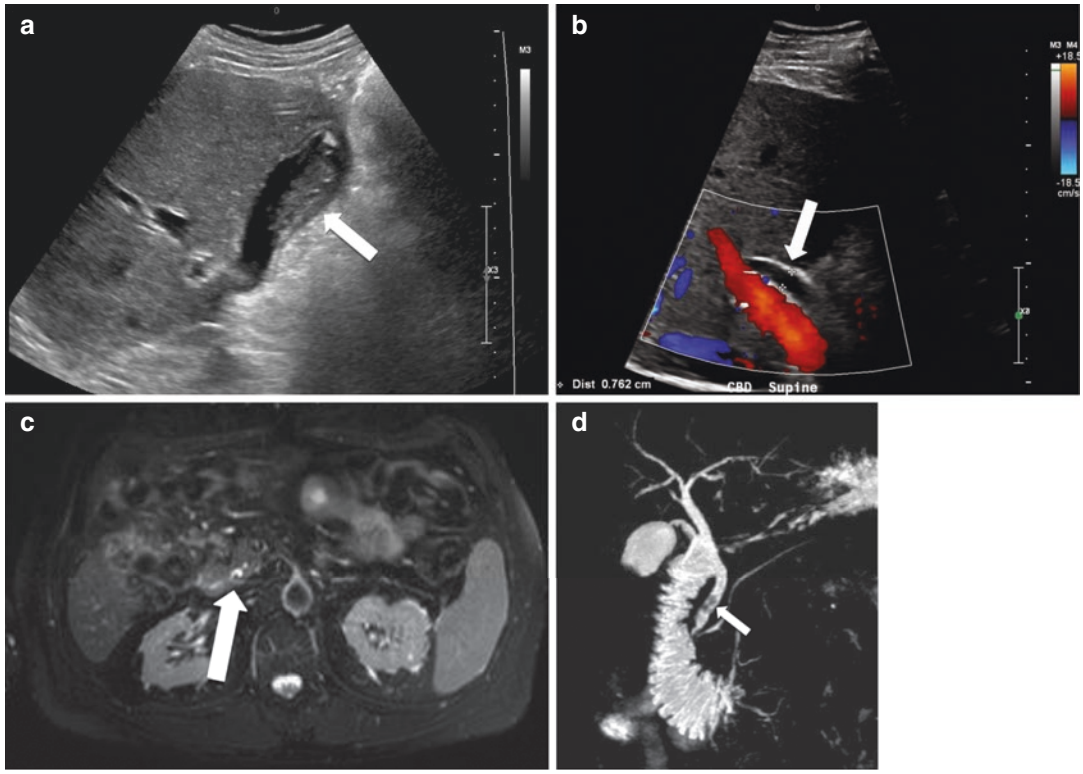

Fig. 4.20 Cholelithiasis and choledocholithiasis. 62-year-old man with right upper quadrant pain. Initial ultrasound performed shows cholelithiasis without cholecystitis (arrow, **a**), and a dilated common bile duct (arrow, **b**). The patient underwent an MRCP given his biliary colic and dilated common bile duct. Axial T2-weighted fat-saturated (**c**) and 3D MRCP images (**d**) reveal calculi in the distal common bile duct (arrows)

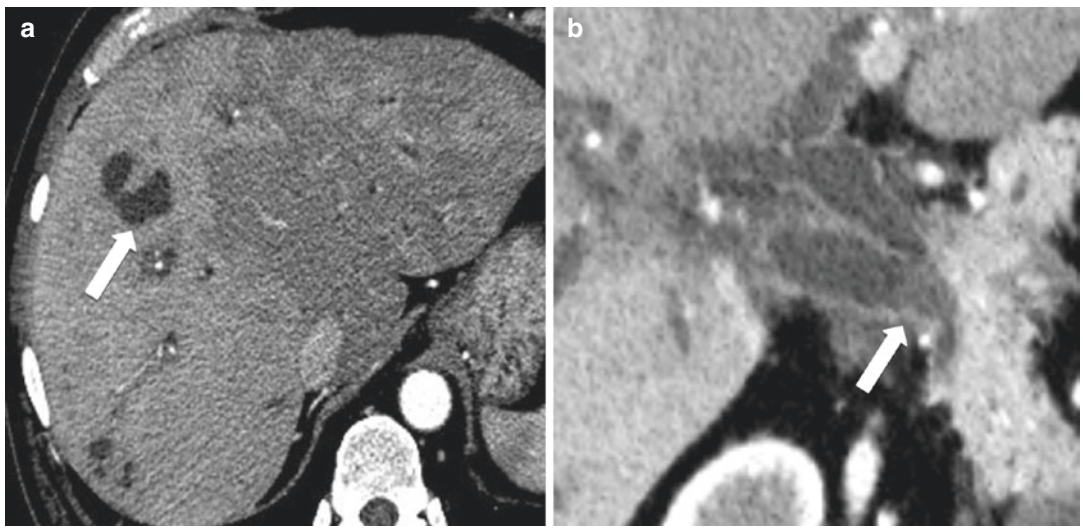

Fig. 4.21 Ascending cholangitis caused by Mirizzi's syndrome. 38-year-old man presents with right upper quadrant pain and fever. Axial (**a**) IV contrast-enhanced CT image show heterogeneous enhancement of the liver parenchyma, dilated intrahepatic bile ducts, and multiple liver abscesses (arrow). Coronal (**b**) IV contrast-enhanced CT image reveals dilatation of the cystic duct and common hepatic duct caused by obstruction by a noncalcified calculus (arrow) located at the junction of both ducts. Also note thickening and hyperenhancement of the biliary duct walls

4.4.3 Recurrent Pyogenic Cholangitis

Recurrent pyogenic cholangitis is caused by pigment calculus formation in the biliary tract, which is thought to be related to parasite infection with *Ascaris lumbricoides* or *Clonorchis sinensis* [36]. The proposed pathophysiology is that parasitic organisms are infesting the biliary tract, and inducing inflammatory and fibrotic changes in the bile duct walls, leading to strictures, bile stasis, disproportional dilation of the extrahepatic bile ducts, intrahepatic calculi, and progressive biliary obstruction with recurrent infection, leading to multiple cholangitic hepatic abscesses, and even cirrhosis (Figs. 4.22 and 4.23) [36]. Parasitic biliary infections are an established risk factor for cholangiocarcinoma [37].

4.5 Acute Traumatic and Iatrogenic Injury to the Biliary Tract

4.5.1 Traumatic Injury

In the setting of trauma, biliary injury is intimately associated with multiple organ injuries: 91% in hepatic injuries, 54% in splenic injuries, and 54% in duodenal injuries [38]. As such, when these injuries are identified, the radiologist must actively search for signs of gallbladder, common bile duct, and intrahepatic bile duct injury, and make recommendations for additional imaging accordingly. Identification of biliary tract injuries in the setting of trauma poses a diagnostic challenge, as these injuries are easily overlooked if there is multi-organ injury. Mechanisms of injury include torsion, shearing, compression, blunt injury, acute deceleration, and penetrating trauma. Although bile duct injuries are rare, occurring in approximately 0.1% of trauma patients, and usually do not pose an imminent threat to life, delayed diagnosis results in high morbidity and mortality from complications including bile leak and superinfection. In the setting of missed diagnosis, symptoms are usually not present until bile is superinfected, resulting in delayed, vague symptoms including abdominal pain, nausea, and vomiting. Laboratory findings may demonstrate rising or persistently elevated bilirubin.

Bile duct injury may involve the intra- or extrahepatic bile ducts, and can be seen as tear or transection, with a frequency of 0.5–21% after hepatic trauma [39]. Injury to the intrahepatic ducts is commonly seen with liver injuries, and usually affects small, subsegmental ducts. Extrahepatic injuries (which include the common hepatic duct and common bile duct) are less frequent, but require treatment with percutaneous, endoscopic, or surgical interventions. Major ducts are usually injured extrahepatically near the hilum due to anatomic fixation due to shear from deceleration or blunt trauma. Many intrahepatic injuries are self-limiting, as they are contained by surrounding liver parenchyma. In a study conducted at our institution, 28% of patients who sustained liver injuries were found to have contained and/or free bile leaks, so the incidence of hepatobiliary injury may be higher than previously thought [40].

In the era of increasing nonoperative management of trauma patients and damage-control surgery with perihepatic packing for liver injuries, open abdomen with subsequent staged surgeries, and decreased use of resection with closing laparotomy and drain placement, identification of a bile leak may be delayed or even go unrecognized for months to years [41]. Patients may present with signs or symptoms of bile leak or bile duct transection or ligation, including jaundice, biliary peritonitis, and cholangitis. However, diagnosis is frequently delayed due to nonspecific symptoms, including abdominal pain, malaise, nausea, and anorexia, which may be attributed to other more frequent postoperative complications [42]. Late manifestations include recurrent cholangitis and secondary biliary cirrhosis due to strictures. Early diagnosis of bile leaks after trauma has been shown to result in a shorter hospital length of stay, with imaging playing an integral role in decreasing morbidity and mortality [43].

A multimodality approach is often warranted to care for these complex patients. There is absence of consensus both in the literature and in

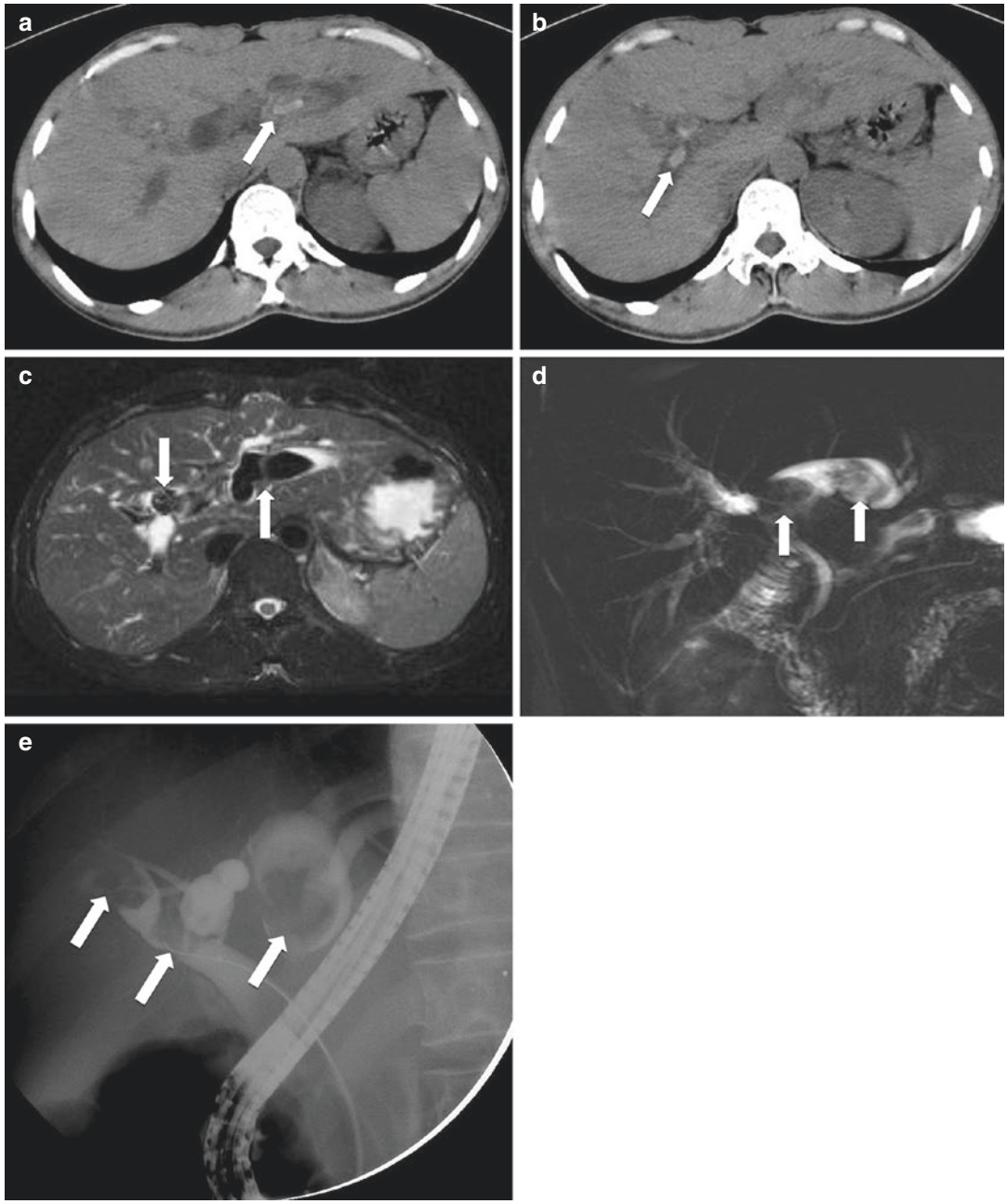

Fig. 4.22 Recurrent pyogenic cholangitis. 46-year-old Asian man who presented with abdominal pain radiating to the back. A non-contrast urinary calculus protocol CT was obtained. Axial images (**a**, **b**) from this examination reveal diffuse, relatively marked intrahepatic bile duct dilation with numerous large intraductal calculi (arrows). Axial T2-weighted fat-saturated (**c**) and 3D MRCP (**d**) images show the same findings (arrows). The patient underwent ERCP (**e**) for calculus extraction and sphincterotomy. Again seen is extensive bile duct dilation, greater in the left hepatic lobe, with multiple bile duct calculi (arrows). These findings are characteristic of recurrent pyogenic cholangitis

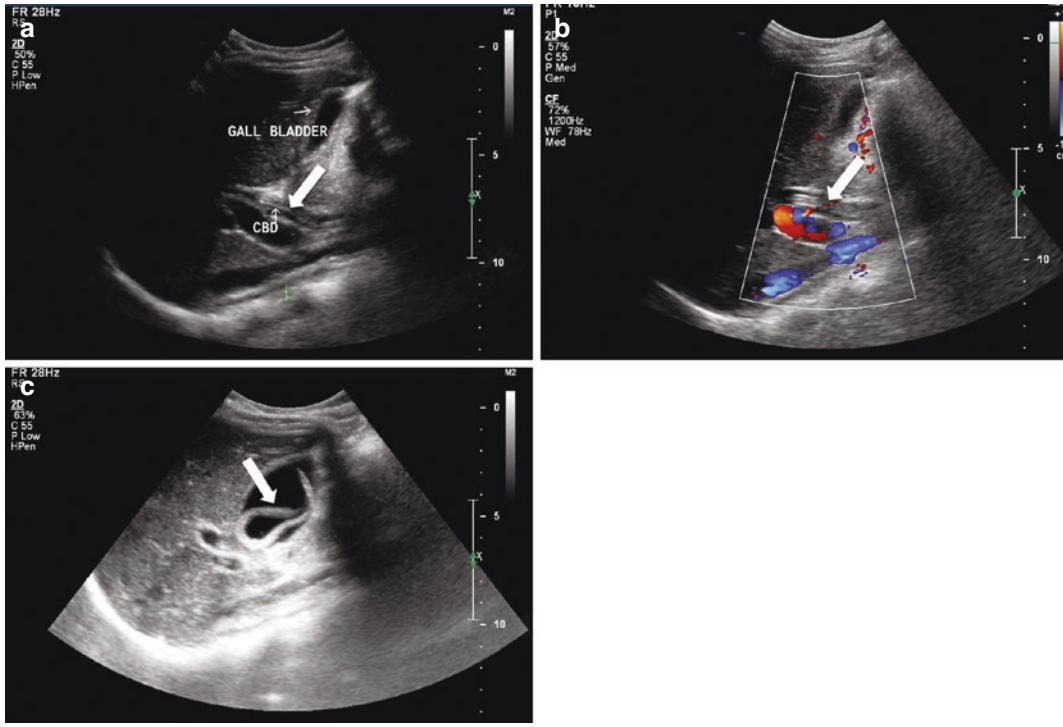

Fig. 4.23 Biliary ascariasis. 22-year-old man from India with right upper quadrant pain. Grayscale (**a**, **c**) and color Doppler (**b**) longitudinal ultrasound images reveal linear and curvilinear echogenic, non-shadowing structures within the common bile duct (arrows in **a**, **b**) and gallbladder (arrow, **c**). Biliary ascariasis was confirmed at ERCP (not shown) (images courtesy of Dr. Tharakeswara Bathala)

practice for an algorithmic approach to the diagnosis of posttraumatic bile leaks. To our knowledge, decisions are often based on the extent of the biliary injury, associated organ injuries, and local expertise. Hemodynamically stable patients who have sustained blunt trauma often undergo CT at the time of admission to delineate their injuries and triage their management. If there is a low suspicion for a bile leak and anatomic detail of the biliary tract is not necessary, hepatobiliary scintigraphy is appropriate for excluding a bile leak. At our institution, our surgical colleagues routinely order hepatobiliary scintigraphy 3–4 days after liver injury. Conversely, if there is a high clinical suspicion for biliary injury including rising serum albumin levels, increasing ascites, enlarging perihepatic fluid collections, or central liver lacerations, MRCP with hepatobiliary contrast material is obtained to provide both anatomic and functional information, which helps guide treatment.

4.6 Iatrogenic Injury

Due to advances in both open and laparoscopic techniques in the last few decades, there has been an increase in the number of hepatobiliary surgeries, including open and laparoscopic cholecystectomy, hepatic resection, and hepatic transplantation, as well as liver biopsy. As a result, there has been a rise in the number of biliary injuries, including bile leak, transection, stricture (Fig. 4.24), and obstruction by surgical clips, which can lead to the development of bilomas, biliary peritonitis, cholangitis, sepsis, biliary cirrhosis, portal hypertension, and hepatic or multi-organ failure.

Detection of biliary injury in the iatrogenic setting is difficult as the patients' clinical symptoms are often nonspecific, including abdominal pain, malaise, nausea, and anorexia, which are frequently seen in association with other more

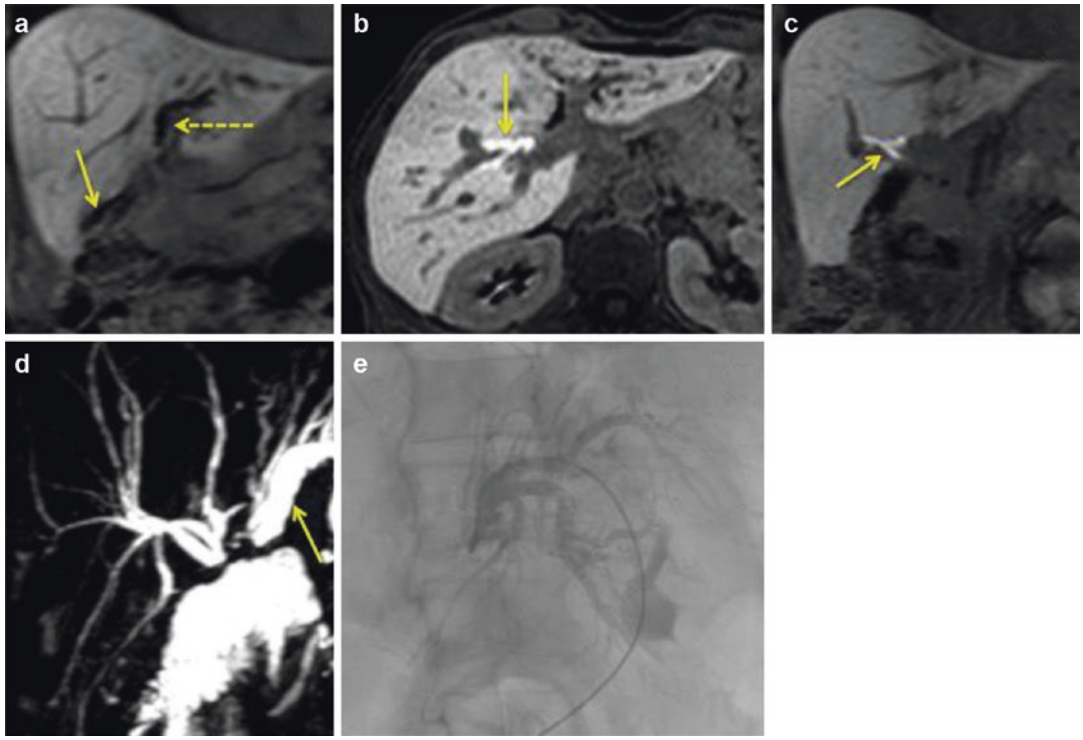

Fig. 4.24 Hepatico-jejunostomy anastomotic stricture. 46-year-old woman with a history of hepatico-jejunostomy now presents with abdominal pain and hyperbilirubinemia. 3D fast spin-echo (3DFSE) MR images demonstrate dilated intrahepatic bile ducts with independent anastomoses of the right (arrow, **a**) and left hepatic ducts (**a**; dashed arrow). On the post-contrast delayed-phase images following the administration of a hepatobiliary contrast agent, the right hepatic duct is shown to be patent (arrow, **b** and c), while the left is obstructed (arrow, **d**). The patient subsequently underwent drainage of the left system via percutaneous transhepatic cholangiography (**e**). Abdom Radiol, Iatrogenic, blunt, and penetrating trauma to the biliary tract, vol 42, 2017, 28–45, LeBedis CA, Bates DDB, Soto JA.

commonly encountered postoperative complications [42, 44]. The reported rates of bile duct injury are 0.3–0.72% for laparoscopic cholecystectomy, 0.1–0.2% for open cholecystectomy, and 2–25% for orthotopic liver transplantation or hepatic resection, particularly in nonanatomic hepatic resections. Only approximately 25% of bile duct injuries are identified intraoperatively [45, 46]. In addition, intraoperative cholangiography is no longer commonly performed due to risk of a tear at the confluence of the cystic and common bile duct at the site of ligation, increased operative time, and increased procedural cost [47]. Thus, a high index of suspicion must be maintained postoperatively for biliary injury.

4.7 Biliary Tract Injury Imaging

Imaging plays a crucial role in the diagnosis of bile duct injury, as well as assessment of its location and severity. A multimodality imaging approach to biliary injury is often necessary, as each modality has its own strengths and limitations. Options include US, CT, MRCP, hepatobiliary scintigraphy, percutaneous transhepatic cholangiography (PTC), and fluoroscopy with a contrast agent injected through a surgically or percutaneously placed biliary drainage catheter [48]. CT is routinely used as the first-line imaging modality in the setting of trauma and the ill postoperative patient, often showing subtle and nonspecific findings associated with

posttraumatic or iatrogenic biliary injury. Liver lacerations, focal perihepatic or intrahepatic fluid collections, and ascites may be the only indicators of bile duct injury. A high level of suspicion is required in the presence of these findings, particularly when other organ injuries (liver, spleen, and duodenum) are noted in the trauma patient, or in the persistently ill postsurgical patient. In these patients, recommending follow-up imaging is essential for the diagnosis of potential late biliary leaks. For example, persistent or increasing low-attenuation intraperitoneal fluid in the setting of recent trauma (Figs. 4.25 and 4.26) or surgery is concerning for bile leakage. Additional findings of peritoneal thickening and hyperenhancement are suggestive of bile peritonitis, and a site of leak should be searched for with advanced imaging modalities [49].

US may be useful in follow-up of known complication to show increasing or decreasing perihepatic fluid, and as a quick and convenient imaging modality for routine follow-up assessment in nonoperative management of hepatic trauma, to detect or confirm the absence of bile leak-related complications [50]. Possible findings in the setting of biliary injury include gallbladder wall thickening, collapsed gallbladder in the setting of perforation, perihepatic and intrahepatic fluid collections, and ascites. More advanced imaging modalities are increasingly recommended and used, as a normal MRCP essentially excludes bile duct injury. When results are indeterminate

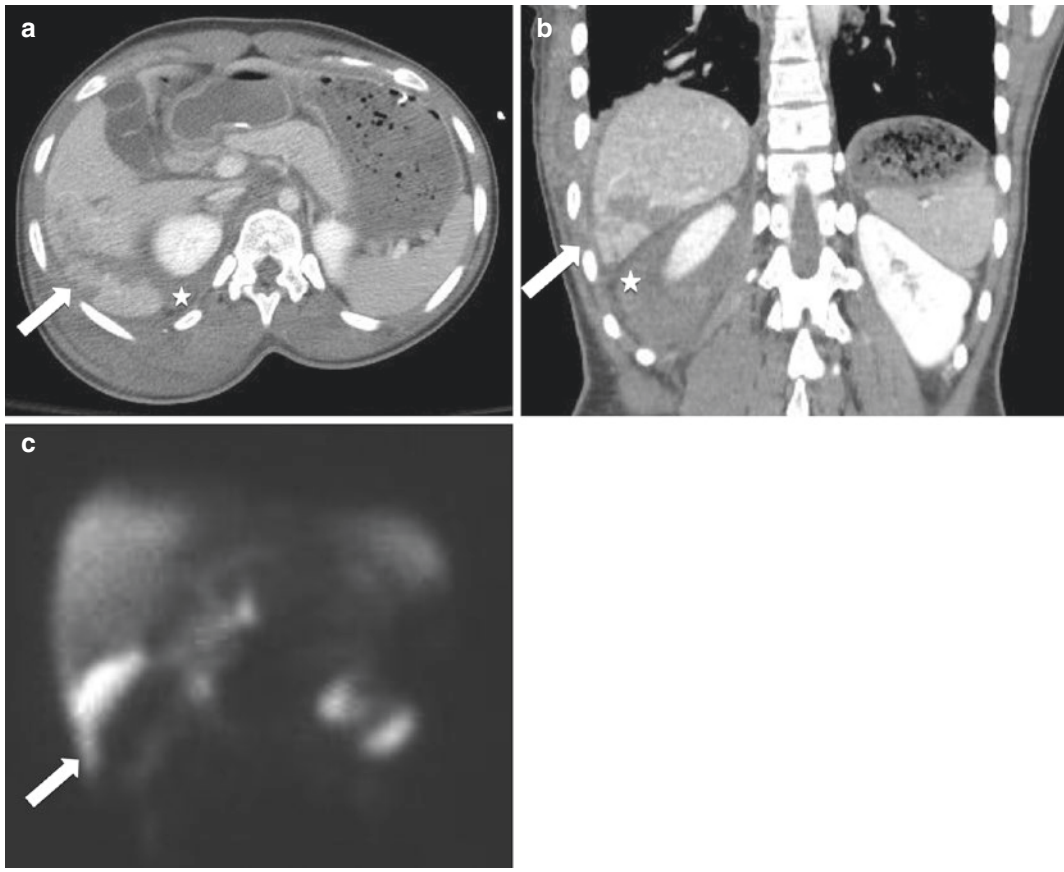

Fig. 4.25 Bile leak due to liver laceration from blunt trauma. 21-year-old woman following a motor vehicle collision who was ejected from her vehicle. Axial (**a**) and coronal (**b**) IV contrast-enhanced CT images reveal an AAST grade 3 laceration (arrows) of segments six and seven with associated perihepatic hemoperitoneum (star). Hepatobiliary scintigraphy (**c**) performed due to concern for a bile leak shows radiotracer extravasating from the liver into the peritoneum (arrow)

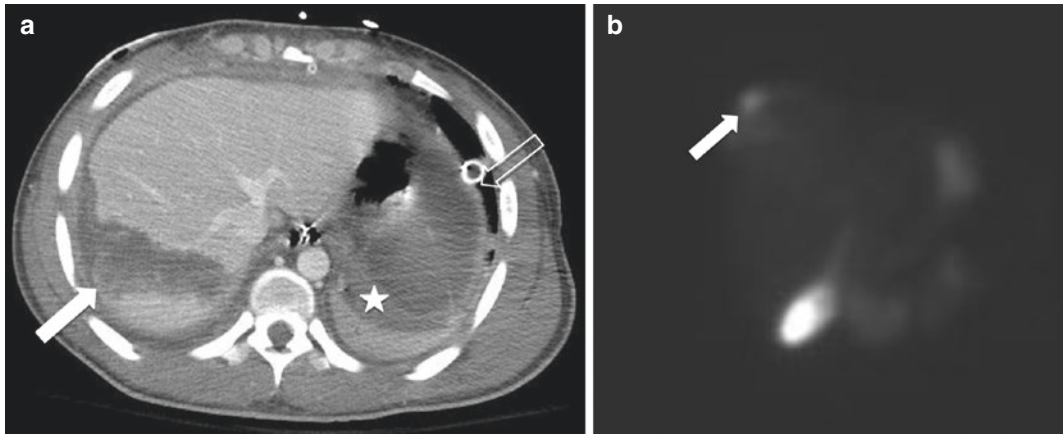

Fig. 4.26 Bile leak due to liver laceration from penetrating trauma. 27-year-man who sustained multiple gunshot wounds to the abdomen and thorax. Axial IV contrast-enhanced CT images show an AAST grade 4 liver laceration at the dome of the liver (**a**, arrow), hemoperitoneum extending into the left upper quadrant (star), and a left chest tube (open arrow). Hepatobiliary scintigraphy (**b**) was subsequently performed, revealing a contained biloma at the site of the laceration at the dome of the liver (arrow)

due to artifacts from peritoneal fluid or tissue edema, hepatobiliary scintigraphy or ERCP may prove definitive in diagnosis.

MRCP with hepatocellular contrast agents provides detailed anatomic information, as well as functional information, with the added advantage of potentially showing the exact site of bile leak and safely permitting differentiation between fluid of biliary and non-biliary origin. MRCP with hepatocyte-selective agents, including gadoxetic acid, can be performed as the initial imaging examination, as it can be used to guide subsequent management, whether it be endoscopic, percutaneous, or surgical [51]. Gadoxetic acid causes T1 shortening of bile, and in conjunction with an MRCP may help in revealing biliary anatomy and bile leaks (Fig. 4.27).

Hepatobiliary scintigraphy provides physiologic information, and is sensitive for demonstrating a bile leak, but delayed 4-h imaging is essential. However, decreased spatial resolution limits the ability to accurately reveal the site of leak, information which governs treatment decisions; thus, evaluation with additional modalities including MRCP and ERCP is commonly needed.

Endoscopic retrograde cholangiopancreatography (ERCP) has both diagnostic and therapeutic capabilities, and remained the reference of imaging standard for decades for biliary tract imaging and intervention. In recent years, ERCP has been commonly reserved solely for patients requiring therapeutic intervention, as imaging modalities have substantially advanced to become the standard diagnostic option for accurate diagnosis [52]. ERCP is more invasive, and is usually pursued after noninvasive imaging examinations have shown or revealed findings suspicious of or definitive for a bile duct injury. Treatment options during the procedure include stenting to bypass and secondarily heal the injury by diverting bile flow with or without sphincterotomy. Another consideration with sphincterotomy is the inherent short-term risk of pancreatitis and a long-term risk of stricture, especially in young patients [53]. The optimal duration of biliary stenting remains to be elucidated to our knowledge, and has been reported to vary from 3 to 16 weeks in prior reports [39, 54].

Percutaneous transhepatic cholangiogram (PTC) and fluoroscopy via an indwelling catheter are useful techniques to guide percutaneous transhepatic biliary drain (PTBD) placement, which can provide biliary drainage and/or diversion in the setting of biliary injury [46]. Compared with ERCP, PTC has the advantage of being able to demonstrate the proximal biliary tract, common bile duct, and, if present, an aberrant right hepatic duct [46].

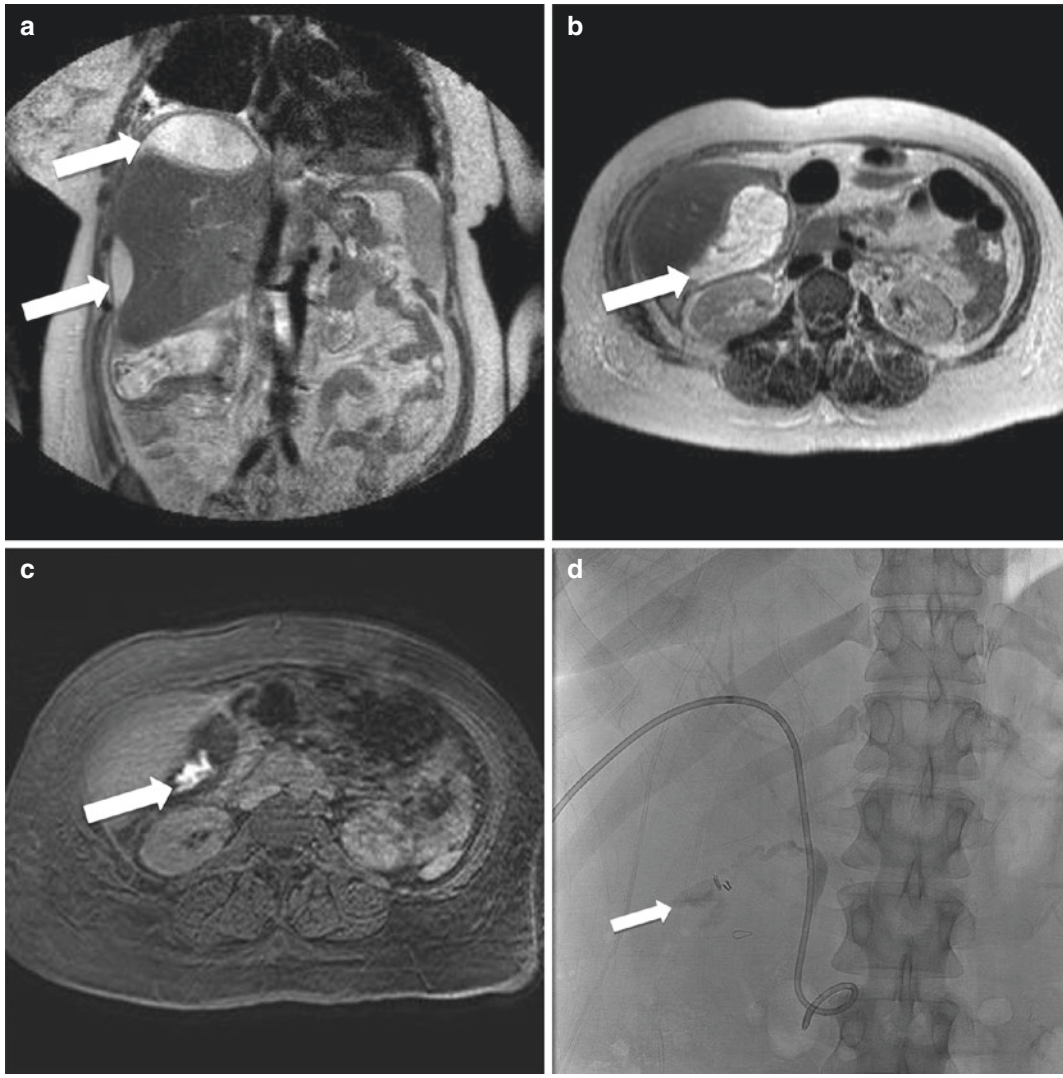

Fig. 4.27 Bile leak after cholecystectomy. 32-year-old woman with worsening abdominal pain 10 days after cholecystectomy. Coronal (**a**) and axial (**b**) T2-weighted MR images demonstrate large perihepatic fluid collection (arrow). Axial T1-weighted gadoxetate disodium-enhanced 20-min delayed MR image (**c**) demonstrates direct leakage of biliary contrast from the cystic duct into the perihepatic fluid collection (arrow). The patient underwent placement of a percutaneous transhepatic biliary drain placement. During this procedure, contrast extravasation confirmed a leak from the cystic duct remnant (arrow, **d**)

4.8 Biloma

A bile leak occasionally results in a biloma which may be intra- or extrahepatic. Since bile is sterile and is absorbed by the peritoneum, patients may not experience any symptoms for weeks after the initial trauma. If the bile becomes superinfected, patients may present with systemic inflammatory response syndrome (SIRS) and respiratory distress [55]. If the biloma results in extrahepatic biliary duct compression, laboratory evaluation may show signs of cholestasis (i.e., elevation of serum alkaline phosphatase, total and direct bilirubin) [55].

In the setting of abdominal trauma, studies report up to a 20% incidence of biliary ascites or bilomas in patients treated conservatively [43, 56]. Bilomas are most commonly described post-iatrogenic injury from cholecystectomy or partial hepatectomy, with an incidence of <0.1% [55]. Other less common causes of biloma include cholangiocarcinoma, acute cholecystitis, tuberculosis, hepatic abscess, infarction, and, rarely, choledocholithiasis in the setting of spontaneous rupture of the biliary tree.

US may have a role in patients with a history of recent trauma or hepatobiliary surgery who present with right upper quadrant pain, chills, and fever, and shows a well-circumscribed, anechoic fluid collection increased through transmission, debris, or septations, in a subphrenic, subhepatic, or intrahepatic location [55]. Loculated ascites or other postoperative collections may appear identical to a biloma, and the need for more advanced imaging or fluid sampling is usually warranted. CT reveals progressive growth of a well-circumscribed, low-attenuation perihepatic or intraparenchymal fluid collection. There should be no identifiable capsule or peripheral enhancement which would indicate a nontraumatic liver mass such as a liver abscess or hemangioma. A hepatic hematoma would also be higher attenuation (as that of blood between 30 and 60 HU, depending on acuity).

Hepatobiliary scintigraphy, MR with hepatobiliary contrast agents, or aspiration may be used for differentiation. MR shows a well-defined fluid collection, which is hyperintense on T2-weighted images and hypointense on T1-weighted images. Hepatobiliary contrast agents are excreted into the biliary tract, and may reveal the site of a bile leak in the hepatobiliary phase. Standard MRCP without hepatobiliary contrast cannot definitively reveal the site of bile leak or be used to distinguish biloma from other fluid collection. Hepatobiliary scintigraphy, if positive, shows focal accumulation of radiotracer outside the biliary tract and bowel. In summary, a loculated low-density collection following hepatic trauma or surgery requires further evaluation.

4.9 Biliary Fistulas

Fistulas are abnormal communications between two epithelial-lined surfaces. Biliary fistulas result from communication of the biliary tract with duodenum, colon, bronchi, skin, or even a vessel. Biliary fistulas most commonly result from gallstone erosion through the gallbladder wall. Trauma and iatrogenic injury may also result in biliary fistulas. The type of fistula will be dictated by the underlying injury and its anatomic relation to surrounding structures.

Biliary-enteric fistula is suggested by pneumobilia, which is detected as gas extending peripherally along the portal triads of the liver within the biliary system. This may be seen on all types of imaging, and must be suggested in the absence of prior sphincterotomy, surgical bypass procedure, recent endoscopic retrograde cholangiopancreatography, or passed common duct calculus [57]. In general, cholecystoduodenal fistulas are the most common type, followed by cholecystocolic and choledochoduodenal fistulas [58]. The clinical manifestation of enterobiliary fistulas is often nonspecific, and most patients are diagnosed on the basis of an incidentally detected imaging finding [58].

Biliary-vascular fistulas are rare, but may be suggested on CT when opacification of the biliary system with iodinated contrast is noted, a finding which is rarely diagnosed prospectively. Diagnosis is most commonly suggested by clinical findings suggesting bleeding, or laboratory evaluation showing excessively high serum levels of direct bilirubin, and only moderately elevated liver enzymes indicating bilhemia (bile mixing with blood). Confirmation is done with selective hepatic arteriography, which shows extravasation of contrast material into the biliary tract, and also serves to exclude hepatic artery aneurysm/pseudoaneurysm as a source of bleeding.

Pleural-biliary fistula may be suspected in nonresolving low-density pleural effusion in the setting of trauma or hepatobiliary surgery (Fig. 4.28). This is typically diagnosed with thoracentesis.

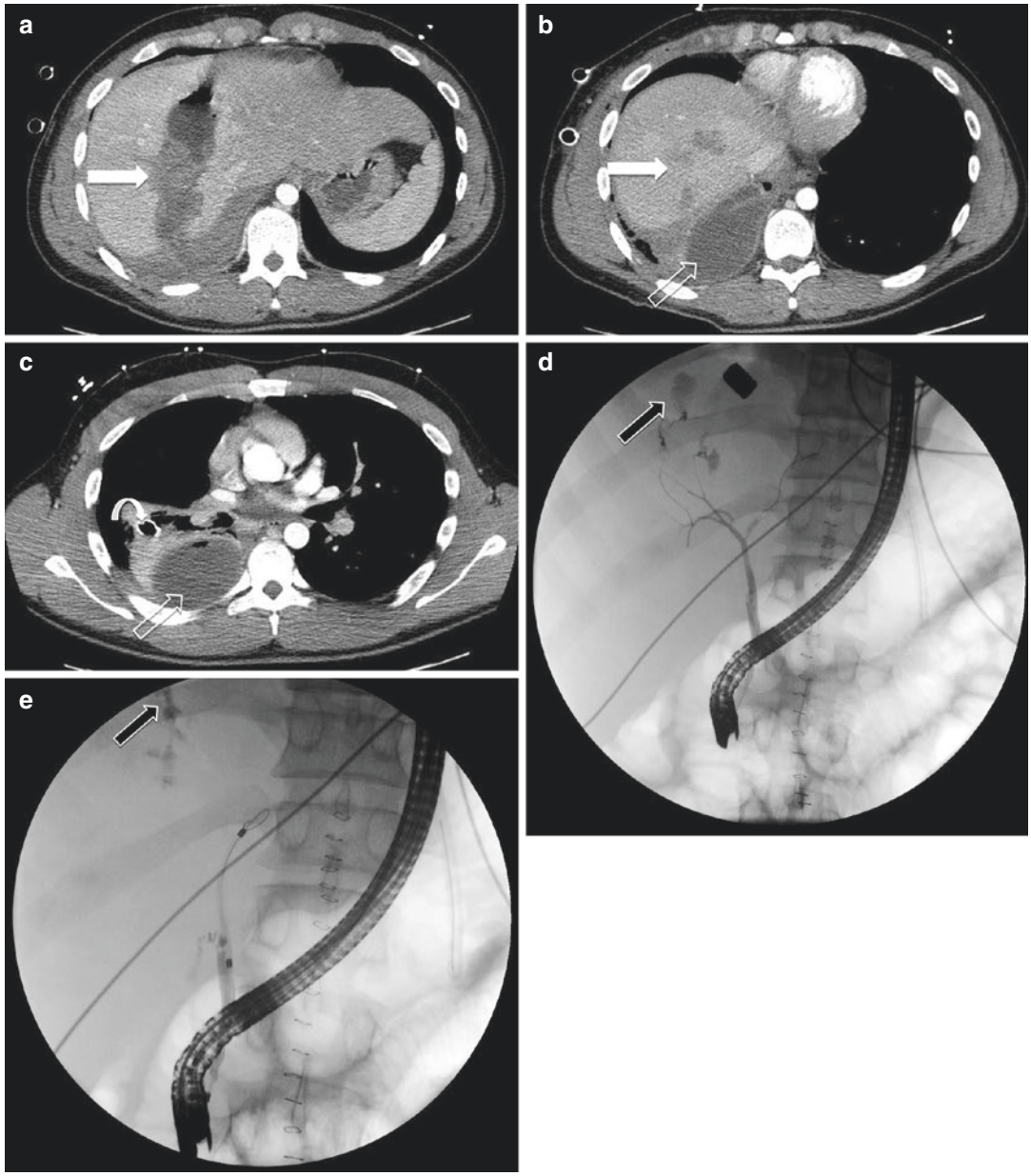

Fig. 4.28 Biliary fistula. 20-year-old man following a gunshot injury, with liver laceration and associated bile leak into the right pleural space. IV contrast-enhanced axial CT images from inferior to superior (**a–b**) reveal an AAST grade 4 liver laceration in the right lobe of the liver along the bullet trajectory (solid arrows), and a right pleural fluid collection (open arrow) with a drainage catheter in place (curved arrow). ERCP images (**d** and **e**) show contrast (arrows) accumulating in the right subphrenic space, and tracking to the right pleural space

4.10 Gallbladder Trauma

Gallbladder injuries include wall contusion, perforation, and avulsion, most of which present as intraluminal or pericholecystic hematoma. Only approximately 2% of patients who undergo laparotomy for traumatic injury are found to have a gallbladder injury [59]. Clinically, a patient with gallbladder injury will develop slowly progressive abdominal complaints, as seen with other traumatic biliary injuries. CT is the first-line

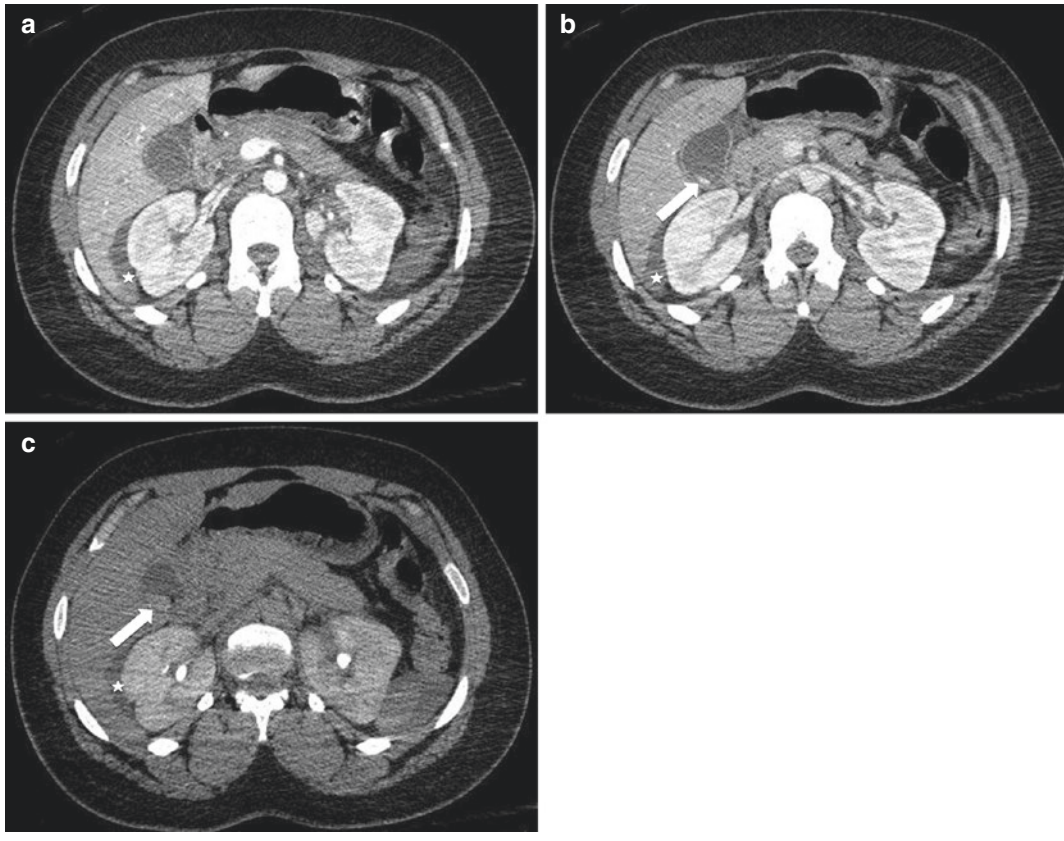

Fig. 4.29 Active gallbladder hemorrhage after blunt trauma. 31-year-old man following rollover motor vehicle collision. Axial IV contrast-enhanced CT images in the arterial (**a**), portal venous (**b**), and 5-min delayed phases demonstrate a focus of hyperattenuation within the gallbladder lumen (arrows in **b** and **c**), which first appears on the portal venous phase, and which expands on the 5-min delayed phase, representing active intraluminal hemorrhage. Perihepatic fluid is also noted (stars)

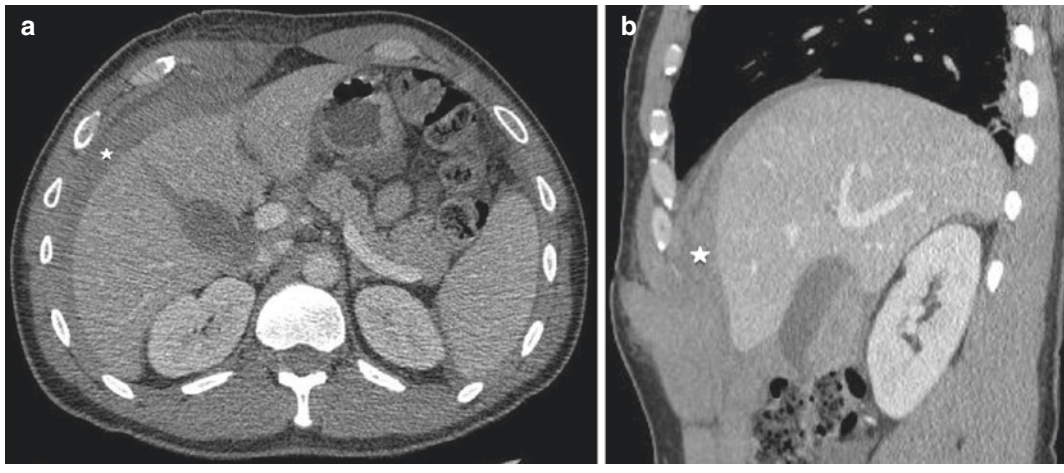

Fig. 4.30 Gallbladder laceration from penetrating trauma. 36-year-old man following stab wound to the right upper quadrant. Axial (**a**) and sagittal (**b**) IV contrast-enhanced CT images show an AAST grade 3 liver laceration extending to the gallbladder wall, and layering hyperattenuating intraluminal material. The patient underwent subsequent cholecystectomy, and a laceration of the gallbladder wall with an associated intraluminal hemorrhage was identified. Perihepatic hematoma was also noted on CT (stars)

imaging modality as it most accurately depicts blood within the gallbladder lumen (Figs. 4.29 and 4.30). Other findings in CT include gallbladder wall thickening, pericholecystic fluid, intramural hematoma or layering blood, indistinct gallbladder wall or discontinuous mucosal enhancement, active bleeding from cystic artery injury, and low-attenuation collections around the liver. An indirect sign of gallbladder wall injury is displacement of the gallbladder from its fossa. US shows echogenic fluid within the gallbladder. Potential mimics of intraluminal blood in the gallbladder on CT include milk of calcium, and vicarious excretion of contrast material from previous CT examinations, which may simulate intraluminal blood [60]. Similar findings are seen with MRI/MRCP. T1-weighted MR images and MRCP aid in identifying intramural hematoma.

Conclusion

A multimodality approach is often warranted to care for patients with hepatobiliary diseases, as they often present as complex diagnostic and therapeutic challenges. In the setting of nontraumatic hepatobiliary injury, as for example with acute cholecystitis, CT and ultrasound remain the imaging examination of choice due to accessibility, low cost, and rapid acquisition. They also serve as useful imaging tools to reveal other causes of acute abdominal pain. High clinical suspicion is often needed to elucidate the more rare presentations of acute abdominal pain, such as a pregnant woman with HELLP syndrome, or a young woman with hemoperitoneum from a ruptured adenoma. In the setting of posttraumatic hepatobiliary injury, there is a lack of consensus, both in the literature and practice, for an algorithmic approach, to our knowledge. Decisions are often based on the extent of biliary injury, associated organ injuries, and local expertise. MRCP often plays an integral role in the diagnosis of posttraumatic complications in stable patients. MRCP is a powerful adjunct imaging tool for equivocal cases, and for showing complications, either from known hepatobiliary disease or in the postoperative setting. It is expected that as MR becomes more advanced in providing accelerated acquisition times, artifact reduction, and cost reduction, it will become a primary imaging modality in emergency hepatobiliary settings where there is a high clinical suspicion for aforementioned diseases and injuries.

References

1. Boll DT, Merkle EM. Diffuse liver disease: strategies for hepatic CT and MR imaging. Radiographics. 2009;29(6):1591–614.
2. Chundru S, Kalb B, Arif-Tiwari H, et al. MRI of diffuse liver disease: characteristics of acute and chronic diseases. Diagn Interv Radiol. 2013;20(3):200–8.
3. Pickhardt PJ, Fleishman MJ, Fisher AJ. Fitz-hugh curtis syndrome: multidetector CT findings of transient hepatic attenuation difference and gallbladder wall thickening. Am J Roentgenol. 2003;180(6):1605–6.
4. Hertzberg B, Middleton W. Ultrasound: the requisites. Philadelphia, PA: Elsevier; 2016. p. 6–68.
5. Semelka R. Abdominal-pelvic MRI. Hoboken, NJ: John Wiley and Sons, Inc.; 2010. p. 418–37.
6. Semelka RC, Kelekis NL, Sallah S, et al. Hepatosplenic fungal disease: diagnostic accuracy and spectrum of appearance on MR imaging. Am J Roentgenol. 1997;169(5):1311–6.
7. Semelka RC, Shoenut JP, Greenberg HM, et al. Detection of acute and treated lesions of hepatosplenic candidiasis: comparison of dynamic contrast-enhanced CT and MR imaging. J Magn Reson Imaging. 1992;2(3):341–5.
8. Oto A, Akhan O, Ozmen M. Focal inflammatory disease of the liver. Eur J Radiol. 1999;32:61–75.
9. Hertzberg B, Middleton W. Ultrasound: the requisites. Philadelphia, PA: Elsevier; 2016. p. 78.
10. Semelka R. Abdominal-pelvic MRI. Hoboken, NJ: John Wiley and Sons, Inc.; 2010. p. 388–98.
11. Brancatelli G, Vilgrain V, Federle MP, et al. Budd-Chiari syndrome: spectrum of imaging findings. Am J Roentgenol. 2007;188(2):W168–76.
12. Torabi M, Hooseinzadeh K, Federle MP. CT of nonneoplastic hepatic vascular and perfusion disorders. Radiographics. 2008;28:1967–82.
13. Valls C, Cos M, Figueras J, et al. Pre-transplantation diagnosis and staging of hepatocellular carcinoma in patients with cirrhosis: value of dual-phase helical CT. Am J Roentgenol. 2004;182(4):1011–7.
14. Mittal S. Epidemiology of HCC: consider the population. J Clin Gastroenterol. 2013;47:s2–6.
15. Semelka R. Abdominal-pelvic MRI. Hoboken, NJ: John Wiley and Sons, Inc.; 2010. p. 189–238.
16. Casillas VJ, Amendola MA, Gascue A, Pinnar N, Levi JU, Perez JM. Imaging of nontraumatic hemorrhagic hepatic lesions. Radiographics. 2000;2:367–78.

17. MacSween R, Anthony P, et al. Pathology of the liver. 3rd ed. London: Churchill Livingston; 1994.
18. Webb WR, Brant WE, Major NM. Fundamentals of body CT. Philadelphia, PA: Elsevier; 2006. p. 225–6.
19. Thomeer MG, Broker M, Verheij J, et al. Hepatocellular adenoma: when and how to treat? Update of current evidence. Ther Adv Gastroenterol. 2016;9(6):898–912.
20. Semelka R. Abdominal-pelvic MRI. Hoboken, NJ: John Wiley and Sons, Inc.; 2010. p. 107.
21. Pritchard JA, Weisma R Jr, Ratnoff OD, Vosburgh GJ. Intravascular hemolysis, thrombocytopenia and other hematologic abnormalities associated with severe toxemia of pregnancy. NEJM. 1954;250:89–98.
22. Sibai BM, Barton JR. Expectant management of severe preeclampsia remote from term: patient selection, treatment, and delivery indications. Am J Obstet Gynecol. 2007;196:514.e1–9.
23. Benedetto C, Marozio L, Tancredi A, et al. Biochemistry of HELLP syndrome. Adv Clin Chem. 2011;53:85–104.
24. Perronne L, Dohan A, Bazeries P, et al. Hepatic involvement in HELLP syndrome: an update with emphasis on imaging features. Abdom Imaging. 2015;40(7):2839–49.
25. O'Connor OJ, Maher MM. Imaging of cholecystitis. Am J Roentgenol. 2011;196(4):W367–74.
26. Soto JA, Lucey BC. Emergency radiology: the requisites. Philadelphia, PA: Elsevier; 2010. p. 334–44.
27. Mirvi S, Kubal W, Shanmuganathan K, et al. Problem solving in emergency radiology. Philadelphia, PA: Elsevier; 2015. p. 452–3.
28. Yang C, Zhang S, Jia Y, et al. Clinical application of dual-energy spectral computed tomography in detecting cholesterol gallstones from surrounding bile. Acad Radiol. 2017;24(4):478–82.
29. Bilgin M, Shaikh F, Semelka RC, Bilgin SS, Balci NC, Erdogan A. Magnetic resonance imaging of gallbladder and biliary system. Top Magn Reson Imaging. 2009;20(1):31–42.
30. Hjartarson JH, Hannesson P, Sverrisson I, Blondal S, Ivarsson B, Bjornsson ES. The value of magnetic resonance cholangiopancreatography for the exclusion of choledocholithiasis. Scand J Gastroenterol. 2016;51(10):1249–56.
31. Soto JA, Lucey BC. Emergency radiology: the requisites. Radiology. 2010;257(2):334.
32. Genevieve BL. CT findings in acute gangrenous cholecystitis. Am J Roentgenol. 2002;178:275–81.
33. Bates D, et al. Use of MR in pancreaticobiliary emergencies. Magn Reson Imaging Clin N Am. 2016;24(2): 422–48.
34. Webb WR, Brant WE, Major NM. Fundamentals of body CT. Philadelphia: Elsevier; 2006. p. 233–46.
35. Liu TH, Consorti ET, Kawashima A, Tamm EP, Kwong KL, Gill BS, Sellin JH, Peden EK, Mercer DW. Patient evaluation and management with selective use of magnetic resonance cholangiography and endoscopic retrograde cholangiopancreatography before laparoscopic cholecystectomy. Ann Surg. 2001;234:33–40.
36. Hffernan EJ, Geoghegan T, Munk PL, Ho SG, Harris AC. Recurrent pyogenic cholangitis: from imaging to intervention. Am J Roentgenol. 2009;192(1):W28–35.
37. Tyson GL, El-Serag H. Risk factors of cholangiocarcinoma. Hepatology. 2011;54(1):173–84.
38. Gupta A, Stuhlfaut JW, Fleming KW, Lucey B, Soto JA. Blunt trauma of the pancreas and biliary tract: a multimodality imaging approach in diagnosis. Radiographics. 2004;24:1381–95.
39. Winick AB, Waybill PN, Venbrux AC. Complications of percutaneous transhepatic biliary interventions. Tech Vasc Interv Radiol. 2001;4:200–6.
40. Melamud K, LeBedis CA, Anderson SW, et al. Biliary imaging: multimodality approach to imaging of biliary injuries and their complications. Radiographics. 2014;34:613–23.
41. Pachter HL, Knudson MM, Esrig B, et al. Status of nonoperative management if blunt hepatic injuries in a multicenter experience with 404 patients. J Trauma. 1996;40:31–8.
42. Vachhani PG, Copelan A, Remer EM, et al. Iatrogenic hepatopancreaticobiliary injuries: a review. Semin Interv Radiol. 2015;32:182–94.
43. Baghdanian AA, Baghdanian AH, Khalid M, et al. Damage control surgery: use of diagnostic CT after life-saving laparotomy. Emerg Radiol. 2016;23(5):483–95.
44. Lee CM, Stewart L, Way LW. Postcholecystectomy abdominal bile collections. Arch Surg. 2000;135:538–44.
45. Stewart L. Iatrogenic biliary injuries. Surg Clin North Am. 2014;94:297–310.
46. Lau WY, Lai EC, Lau SH. Management of bile duct injury after laparoscopic cholecystectomy. ANZ J Surg. 2010;80:75–81.
47. Fletcher DR, Hobbs MS, Tan P, et al. Complications of cholecystectomy: risks of the laparoscopic approach and protective effect of operative cholangiography: a population-based study. Ann Surg. 1999;229:449–57.
48. Thompson CM, Saad NE, Quazi RR, et al. Management of bile duct injuries: role of the interventional radiologist. Radiographics. 2013;33:117–34.
49. Vassiliu P, Touttouzas KG, Velmahos GC. A prospective study of posttraumatic biliary and pancreatic fistuli.The role of expectant management. Injury. 2004;35:223–7.
50. Chiu WC, Wong-You-Cheong JJ, Rodriguez A, et al. Ultrasonography for interval ssessment in the nonoperative management of hepatic trauma. Am Surg. 2005;71:841–6.
51. Aduna M, Larena JA, Martin D, et al. Bile duct leaks after laparoscopic cholecystectomy: value of contrast-enhanced MRCP. Abdom Imaging. 2005;30:480–7.
52. Bor R, Madácsy L, Fábián A, Szepes A, Szepes Z. Endoscopic retrograde pancreatography: when should we do it? World J Gastrointest Endosc. 2015;7(11):1023–31.
53. Walsh RM, Henderson JM, Vogt DP, et al. Long-term outcome of biliary reconstruction from bile duct injuries from laparoscopic cholecystectomies. Surgery. 2007;142:450–6.

54. Stewart L, Way LW. Laparoscopic bile duct injuries: timing of surgical repair does not influence success rate—a multivariate analysis of factors influencing surgical outcomes. HPB (Oxford). 2009;11:516–22.
55. Tana C, D'Alessandro P, Tartaro A, Tana M, Mezzetti A, Schiavone C. Sonographic assessment of a suspected biloma: a case report and review of the literature. World J Radiol. 2013;5(5):220–5.
56. Croce MA, Fabian RC, Menke PG, et al. Nonoperative management of blunt hepatic trauma is the treatment of choice for hemodynamically stable patients: reports of a prospective trial. Ann Surg. 1995;221: 744–53.
57. Pickhardt PJ, Bhalla S, Balfe DM. Acquired gastrointestinal fistulas: classification, etiologies, and imaging evaluation. Radiology. 2002;224(1):9–23.
58. Inal M, Oguz M, Aksungur E, Soyupak S, Boruban S, Akgul E. Biliary-enteric fistulas: report of five cases and review of the literature. Eur Radiol. 1999;9: 1145–51.
59. Soderstrom CA, Maekawa K. Gallbladder injuries resulting from blunt abdominal trauma: an experience and review. Ann Surg. 1981;193:60–6.
60. Wittenberg A, Minotti A. CT diagnosis of traumatic gallbladder injury. Am J Roentgenol. 2005;185: 1573–4.